THESIS FOR THE DEGREE OF LICENTIATE OF ENGINEERING

Phase-Noise Compensation for Space-Division Multiplexed Multicore Fiber Transmission

Arni F. Alfredsson

CHALMERS
UNIVERSITY OF TECHNOLOGY

Communication Systems Group
Department of Electrical Engineering
Chalmers University of Technology
Göteborg, Sweden, 2018

Phase-Noise Compensation for Space-Division Multiplexed Multicore Fiber Transmission

Arni F. Alfredsson

Technical Report No. R013/2018
ISSN 1403-266X

This thesis has been prepared using LaTeX and Tikz.

Communication Systems Group
Department of Electrical Engineering
Chalmers University of Technology
SE-412 96 Göteborg, Sweden
Phone: +46 (0)31 772 17 42
www.chalmers.se

Front cover illustration:
Correlated phase noise in 3 cores of a multicore fiber.
Based on the experimental data used in [Paper C].

Printed by Chalmers Reproservice
Göteborg, Sweden, September 2018

Abstract

The advancements of popular Internet-based services such as social media, virtual reality, and cloud computing constantly drive vendors and operators to increase the throughput of the Internet backbone formed by fiber-optic communication systems. Due to this, space-division multiplexing (SDM) has surfaced as an appealing technology that presents an opportunity to upscale optical networks in a cost-efficient manner. It entails the sharing of various system components, such as hardware, power, and processing resources, as well as the use of SDM fibers, e.g., multicore fibers (MCFs) or multimode fibers, which are able to carry multiple independent signals at the same wavelength in parallel.

Higher-order modulation formats have also garnered attention in recent years as they allow for a higher spectral efficiency, an important parameter that relates to the throughput of communication systems. However, a drawback with increasing the order of modulation formats is the added sensitivity to phase noise, which calls for effective phase-noise compensation (PNC). This thesis studies the idea of sharing processing resources to increase the performance of PNC in SDM systems using a particular type of fiber, namely uncoupled, homogeneous, single-mode MCF.

Phase noise can be highly correlated across channels in various multichannel transmission scenarios, e.g., SDM systems utilizing MCFs with all cores sharing the same light source and local oscillator, and wavelength-division multiplexed systems using frequency combs. However, the nature of the correlation in the phase noise depends on the system in question. Based on this, a phase-noise model is introduced to describe arbitrarily correlated phase noise in multichannel transmission. Using this model, two pilot-aided algorithms are developed using i) the sum–product algorithm operating in a factor graph and ii) variational Bayesian inference. The algorithms carry out joint-channel PNC and data detection for coded multichannel transmission in the presence of phase noise. Simulation results show that in the case of partially-correlated phase noise, they outperform the typical PNC approach by a wide margin. Moreover, it is shown that the placement of pilot symbols across the channels has a considerable effect on the resulting performance.

Focusing on SDM transmission through an uncoupled, homogeneous, single-mode MCF with shared light source and local oscillator lasers, the performance benefits of joint-channel PNC are investigated. A significant gain in transmission reach is experimentally demonstrated, and the results are shown to agree strongly with simulations based on the introduced phase-noise model. In addition, the simulations show that dramatic improvements can be made for phase-noise limited systems in terms of power efficiency, spectral efficiency, and hardware requirements.

Keywords: Coherent fiber-optic communications, detection, estimation, multicore fiber, phase noise, space-division multiplexing.

List of Publications

This thesis is based on the following publications:

[A] **A. F. Alfredsson**, E. Agrell, and H. Wymeersch, "Iterative detection and phase-noise compensation for coded multichannel optical transmission," submitted to *IEEE Transactions on Communications*, May 2018.

[B] **A. F. Alfredsson**, E. Agrell, H. Wymeersch, and M. Karlsson, "Pilot distributions for phase tracking in space-division multiplexed systems," in *Proc. European Conference on Optical Communication (ECOC)*, Sep. 2017, p. P1.SC3.48.

[C] **A. F. Alfredsson**, E. Agrell, H. Wymeersch, B. J. Puttnam, G. Rademacher, R. S. Luís, and M. Karlsson, "On the performance of joint-channel carrier-phase estimation in space-division multiplexed multicore fiber transmission," submitted to *Journal of Lightwave Technology*, Aug. 2018.

Publications by the author not included in the thesis:

[D] **A. F. Alfredsson**, R. Krishnan, and E. Agrell, "Joint-polarization phase-noise estimation and symbol detection for optical coherent receivers," *Journal of Lightwave Technology*, Sep. 2016.

[E] **A. F. Alfredsson**, E. Agrell, H. Wymeersch, and M. Karlsson, "Phase-noise compensation for spatial-division multiplexed transmission," in *Proc. Optical Fiber Communication Conference (OFC)*, Mar. 2017, p. Th4C.7.

[F] E. Agrell, **A. F. Alfredsson**, B. J. Puttnam, and R. S. Luís, G. Rademacher, and M. Karlsson, "Modulation and detection for multicore superchannels with correlated phase noise," (invited paper) in *Proc. Conference on Lasers and Electro-Optics (CLEO)*, May 2018, p. SM4C.3.

[G] B. J. Puttnam, R. S. Luís, G. Rademacher, **A. F. Alfredsson**, W. Klaus, J. Sakaguchi, Y. Awaji, E. Agrell, and N. Wada, "Characteristics of homogeneous multicore fibers for SDM transmission," (invited paper) submitted to *APL Photonics*, Jul. 2018.

[H] **A. F. Alfredsson**, E. Agrell, H. Wymeersch, B. J. Puttnam, G. Rademacher, and R. S. Luís, "Joint phase tracking for multicore transmission with correlated phase noise," (invited paper) in *Proc. IEEE Summer Topicals Meeting Series (SUM)*, Jul. 2018, p. MF1.2.

Acknowledgements

I would like to thank Prof. Erik Agrell for his continual support and tolerance for my questions and doubts during this first part of my PhD studies. You have taught me a great deal when it comes to doing research, and I certainly would not be here without you. Moreover, Prof. Henk Wymeersch has been instrumental in my progress and has been especially helpful with all things Bayesian, which I highly appreciate. I would also like to thank Prof. Magnus Karlsson for the discussions we have had over the years, which have given me a lot of insight into fiber-optic communication systems. Finally, I want to thank Dr. Pontus Johannisson for his help in the beginning of my PhD studies.

A big thanks goes to my collaborators at the National Institute of Information and Communications Technology who provided me with experimental data that considerably improved the quality of my work. I want to specifically acknowledge Benjamin Puttnam for his all efforts pertaining to the collaboration, and Ruben Luís for assisting me with the signal processing of the experimental data. I hope we continue our collaboration during the rest of my PhD studies.

Thanks to Prof. Erik Ström for his ambitions in improving the working environment at Chalmers, as well as to the administration staff for their help. Moreover, I want to acknowledge all of my colleagues in the FORCE group for providing a diverse and challenging working environment. Special thanks goes to the people in the CS group for making the workplace awesome.

I am grateful for my family who has always been very supportive. Last but not least, huge thanks goes to Jóhanna for her endless motivation and patience with me. I would not want to do this without you.

Árni F. Alfgeirsson

Göteborg, 2018

Financial Support

This work was supported by the Swedish Research Council (VR) under grants 2013-5642 and 2014-6138. Moreover, I would like to acknowledge Ericsson's Research Foundation for partially funding my research travels.

Acronyms

AWGN	additive white Gaussian noise
BER	bit error rate
BPS	blind phase search
CD	chromatic dispersion
CMA	constant modulus algorithm
DSP	digital signal processing
FEC	forward error correction
FG	factor graph
FIR	finite impulse response
FWM	four-wave mixing
LO	local oscillator
LPN	laser phase noise
MAP	maximum *a posteriori*
MCF	multicore fiber
MIMO	multiple-input multiple-output
MMF	multimode fiber
PDF	probability density function
PDM	polarization-division multiplexing
PMD	polarization-mode dispersion
PMF	probability mass function
PNC	phase-noise compensation
PSK	phase-shift keying
QAM	quadrature amplitude modulation
QPSK	quadrature phase-shift keying
SDM	space-division multiplexing
SMF	single-mode fiber
SNR	signal-to-noise ratio
SPA	sum–product algorithm
SPM	self-phase modulation
VB	variational Bayesian
WDM	wavelength-division multiplexing
XPM	cross-phase modulation

Contents

Part I

Overview

CHAPTER 1

Background

Telecommunications have existed for many centuries and early examples go all the way back to ancient civilizations where information was conveyed using, e.g., smoke signals, mirrors, and drums [1, Pt. 4]. A breakthrough occurred in the 20th century when digital communication systems surfaced and eventually led to a worldwide network called the Internet, which revolutionized the world. The Internet has grown immensely in the last few decades, with the estimated traffic today being more than 20 million times greater than what it was less than three decades ago [2]. Moreover, due to the popularity of modern services such as social media, virtual reality, streaming, and cloud computing, it is still growing at a rapid pace. Fig. 1.1 shows the estimated global Internet traffic per second since 1992 and the predicted rate for 2021.

One of the key enablers of this remarkable growth are fiber-optic communication systems, which today form the Internet backbone due to their enormous throughput capabilities. Broadly speaking, these systems operate by encoding information on light in the near-infrared spectrum and propagating it through an optical fiber. They came into existence in the 1960s with the invention of the laser [3] and optical fiber [4], but worldwide research-and-development efforts did not start until optical fibers with low losses were invented in the 1970s [5]. Since then, the throughput and transmission reach of fiber-optic systems has increased tremendously thanks to a number of technological breakthroughs in the last few decades. This includes the optical amplifier, which was invented in the 1980s [6,7] and was able to extend transmission reach up to thousands of kilometers by periodically compensating for the fiber loss. Wavelength-division multiplexing (WDM) [8] was introduced at a similar time and through the simultaneous transmission of multiple wavelength channels, it enabled the utilization of a much broader wavelength band in

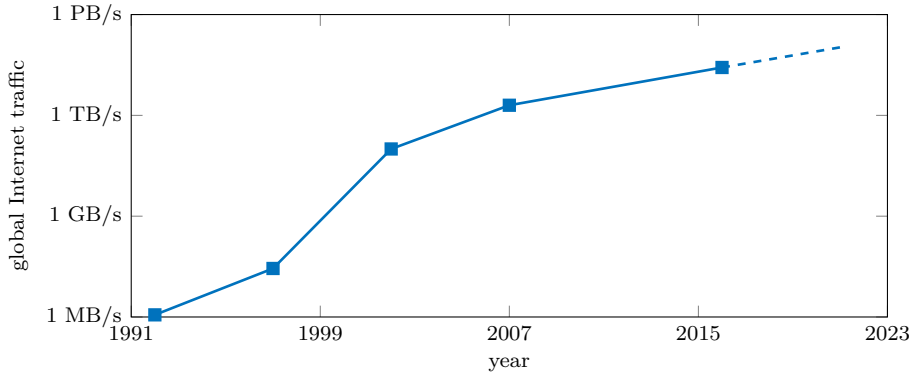

Figure 1.1: The estimated global Internet traffic per second over the past decades and a prediction for 2021 [2].

the optical fiber than was previously possible, which dramatically increased the overall system throughput. Moreover, interest in coherent detection was rekindled[1] in the 2000s after it was recognized that together with digital signal processing (DSP), it enabled the use of various algorithms for effective compensation of transmission impairments, as well as the use of advanced modulation formats and polarization-division multiplexing (PDM) [10, 11]. Hence, all available degrees of freedom (amplitude, phase, polarization, and time) of the optical field became available for information encoding, which in turn allowed for higher data rates and transmission distances compared to noncoherent detection.

As seen in Fig. 1.1, the Internet traffic is expected to continue its exponential growth during the next years due to the ever-increasing popularity of bandwidth-hungry Internet-based services. In the past, advancements in optical amplification and WDM for systems utilizing single-mode fibers (SMFs) sufficed to support the growth in an economical manner, since the amount of data transmitted through the SMF was increased through equipment upgrades [12]. However, as the traffic continues to grow, it is believed that an increasing number of SMFs in optical networks will reach their information-theoretic capacity [13] in the coming years. This fundamental limit is estimated to be about 100–200 Tb/s [12] owing to amplified spontaneous emission, launch power restrictions[2], and optical amplifier bandwidth [15]. Fig. 1.2 shows throughput record demonstrations since 2008 for long-haul transmission over more than 6000 km [16–21] and short-haul transmission over at least 100 km [22–26]. As can be seen, state-of-the-art SMF systems in laboratories have indeed been rapidly approaching the limit, with the current short- and

[1] Coherent detection was initially under active research in the 1980s [9], but its development got abandoned soon after due to the success of optical amplifiers and noncoherent WDM-based systems.

[2] Increasing the launch power beyond a certain point degrades the performance of conventional fiber-optic systems and eventually causes fiber fuse, which has catastrophic effects [14].

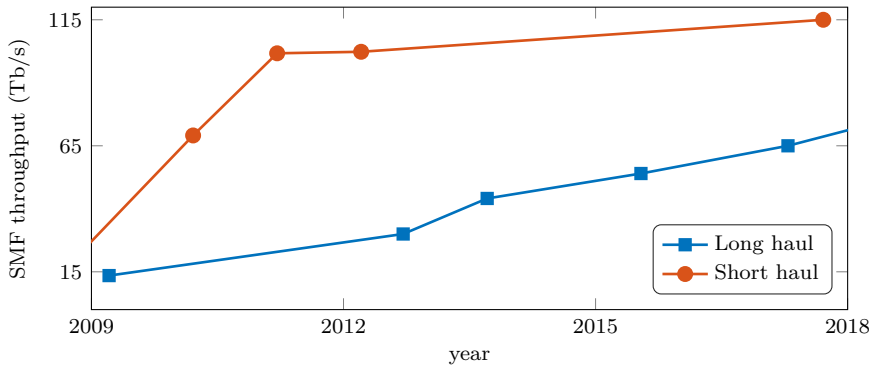

Figure 1.2: Record throughput demonstrations over the past decade for short-haul transmission over more than 100 km and long-haul transmission over more than 6000 km through an SMF.

long-haul throughput records standing at 115.9 Tb/s transmission over 100 km and 71.6 Tb/s transmission over 6970 km, resp. Therefore, the only way to significantly grow the capacity of future optical links is to add more spatial channels [27], and without technological advancements, operators will have to resort to the costly solution of installing new fibers and equipment to keep up with the traffic growth.

The need for increased capacity along with progress in the development of various fibers and system components [28] has initiated worldwide research efforts for space-division multiplexing (SDM) in recent years, albeit the original concept of SDM dates back to the 1970s [29]. The goal of SDM is to upscale optical networks in a cost-effective manner through the simultaneous transmission of spatially distinguishable channels together with the integration of system components and the sharing of resources. In particular, since some transmission impairments will be common among the spatial channels in various SDM systems, DSP resources can be shared, which may reduce the computational complexity of algorithms or improve their performance. Transmission of parallel spatial channels can be realized in several ways, e.g., by utilizing bundles of SMFs or specialized SDM fibers such as multicore fibers (MCFs), multimode fibers (MMFs), and multicore–multimode fibers. The different types of SDM fibers will be discussed in Chapter 4.

In this thesis, we investigate the sharing of DSP resources to improve the performance of phase-noise compensation (PNC) for SDM transmission. First, we develop two pilot-aided algorithms that performs joint-channel PNC for arbitrarily correlated phase noise and any number of channels. To assess their performance, we compare them through simulations with the blind phase search (BPS) algorithm for coded multichannel transmission in the presence of partially-correlated phase noise. Thereafter, we focus on the problem of arranging the pilot symbols across the space and time domain to optimize the performance of joint-channel PNC. Lastly, we introduce a multichannel phase-noise model for transmission through a particular type of SDM fiber, namely an uncoupled, ho-

mogeneous, single-mode MCF, where all cores share the light source and local oscillator (LO) lasers. Using one of the proposed algorithms, we compare the performance of two PNC strategies, namely joint-channel and per-channel processing, in multiple aspects using experimental data and simulations based on the model. In addition, the phase-noise model is validated based on comparisons between simulations and experimental results.

1.1 Thesis Organization

This thesis is divided into two parts, where the first part serves as background material for the second part, which comprises the publications included in the thesis. The first part is organized as follows. Chapter 2 gives an overview of the main signal impairments that occur due to propagation over the fiber-optic channel and imperfections in the coherent transceiver. In addition, typical DSP techniques used to compensate for these impairments and recover the transmitted signal are reviewed. Chapter 3 presents a more detailed background on laser phase noise (LPN) and reviews the problem of optimal bit detection in the presence of this impairment, as well as different DSP algorithms found in the literature that compensate for LPN in both single-channel and multichannel transmission scenarios. This chapter serves as background for Papers A–C. Chapter 4 provides further background material for Papers B–C with a focus on the different types of SDM fibers. Finally, Chapter 5 summarizes the appended publications and discusses possible future work.

1.2 Notation

The notation used in the first part of the thesis as well as the appended publications is as follows. The estimate of a parameter x is represented by $\hat{x}$. Scalars, vectors, and matrices are denoted as x, $\boldsymbol{x}$, and $\mathbf{X}$, resp. An identity matrix of size D is written as $\mathbf{I}_D$ and $\mathrm{diag}(\,\cdot\,)$ denotes a diagonal matrix. Random variables are represented by X, and x denotes their realizations. Probability density functions (PDFs) are denoted by $p_X(x)$ or $p(x)$, whereas probability mass functions (PMFs) are written as $P_X(x)$ or $P(x)$. Mixed discrete–continuous distributions are written the same way as PDFs. More specifically, a multivariate real Gaussian PDF with the mean $\boldsymbol{\mu}$, covariance matrix $\boldsymbol{\Sigma}$, and argument $\boldsymbol{x}$ is denoted as $\mathcal{N}_{\boldsymbol{x}}(\boldsymbol{\mu}, \boldsymbol{\Sigma})$, its complex counterpart with argument $\boldsymbol{z}$ is written as $\mathcal{CN}_{\boldsymbol{z}}(\boldsymbol{\mu}, \boldsymbol{\Sigma})$, and a Tikhonov (or von Mises) PDF with the parameter κ and argument z is denoted by $\mathcal{T}_z(\kappa)$. The expectation of a random variable X with respect to a distribution $P_X(x)$ is denoted as $E_{P_X}[X]$ or simply as $E[X]$, whereas its variance is written as $\mathrm{Var}(X)$. The imaginary number is represented by j, and the real part, imaginary part, complex conjugate, and angle of a complex number are typeset as $\Re\{\,\cdot\,\}$, $\Im\{\,\cdot\,\}$, $(\,\cdot\,)^*$, and $\angle(\,\cdot\,)$, resp. Finally, the transpose of a vector is denoted as $(\,\cdot\,)^T$.

CHAPTER 2

Fiber-Optic Communication Systems

Communication systems that transfer information using light are commonly referred to as optical communication systems (or lightwave systems) and can further be categorized as guided and unguided systems [30, Ch. 1.3]. Unguided systems are also known as free-space optical communication systems, where a light beam that carries information is propagated unconfined through space, similarly to radio communication systems. These systems are the subject of active research and find their use in both short- and long-range applications, with one of the biggest challenges being the Earth's atmosphere scattering the light beams and significantly degrading the transmission performance [31, Ch. 1.1]. Guided systems, on the other hand, operate by propagating a lightwave carrier in a waveguide and are usually implemented using various types of optical fibers. The typical cross section of a standard SMF is depicted in Fig. 2.1. The light propagates through a silica core surrounded by a cladding that confines the light to the core during propagation. Outside of the cladding is a plastic jacket to protect the fiber, and in some applications, additional sturdier layers are used for further protection. This thesis will focus on fiber-optic communication systems, which are used in many scenarios that require high throughput, e.g., long-haul links forming the Internet backbone or short-haul applications such as data centers and passive optical networks.

In short-haul applications, the optical link length is on the order of a few meters up to 100 km. Since the installment and maintenance of these links are costly, noncoherent transmission over MMFs has traditionally been the prevalent strategy for economic reasons [32]. On the other hand, coherent SMF systems are capable of higher spectral efficiencies and transmission reaches compared to noncoherent MMF systems, and have thus become the standard for high-performance long-haul links extending to thousands

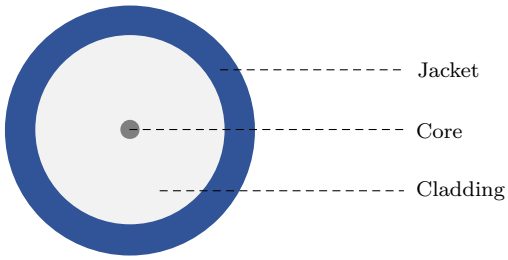

Figure 2.1: The cross section of a standard SMF.

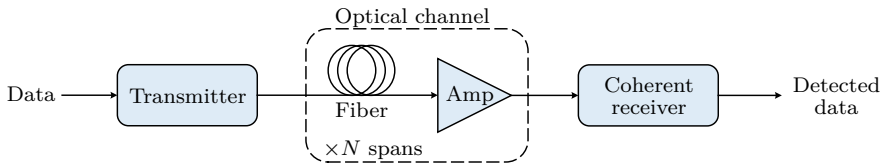

Figure 2.2: High-level view of a typical fiber-optic long-haul link consisting of a transmitter, N spans of an optical fiber and an amplifier, and a coherent receiver.

of kilometers. This is due to coherent systems being able to encode information in the amplitude, phase, and polarization of the optical field, whereas noncoherent systems are limited to modulating only the amplitude of the light. In addition, since coherent receivers have access to the entire optical field, they allow for a more effective impairment compensation using DSP [10]. The focus in this thesis will be on coherent transmission systems.

Fig. 2.2 shows a high-level picture of a fiber-optic long-haul link, i.e., the transmitter, the optical channel, and the coherent receiver. Moreover, considering single-wavelength, PDM transmission through a standard SMF, a typical optical transmitter is depicted in Fig. 2.3. A laser that acts as a light source is split into two beams, and each beam enters two modulators that encode information into the in-phase and quadrature components of the lightwave. The electrical signals that drive the modulators can be generated in various ways, e.g., through the use of DSP and arbitrary waveform generators. The quadrature component is then phase shifted by $\pi/2$ and combined with the in-phase component. Both beams are X-polarized at this point, and hence, one of the beams is polarization rotated to become Y-polarized and combined with the other beam through a polarization beam combiner. This results in a PDM signal that is transmitted and propagated through the optical channel, which comprises N spans, each consisting of an optical amplifier and a fiber span. The coherent optical receiver is shown in Fig. 2.4. The received signal and light from the LO laser are each split into two beams. The beam corresponding to the X-polarization of the received signal enters a 90° optical

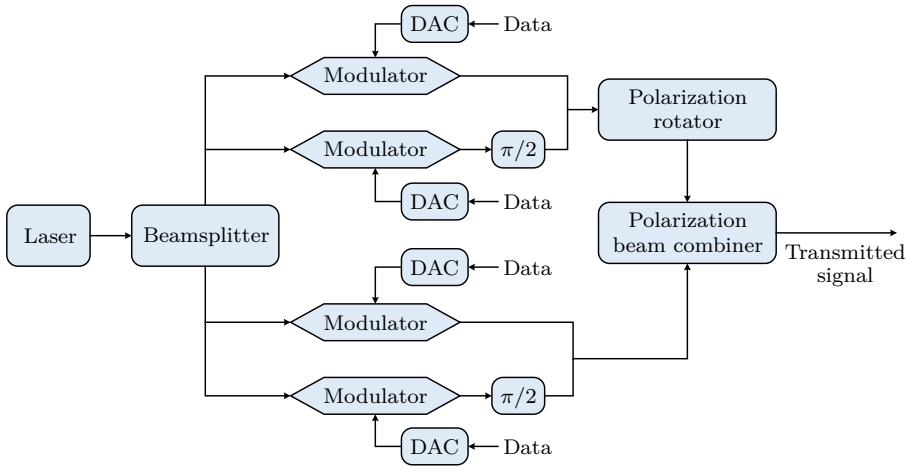

Figure 2.3: Overview of a typical optical transmitter for single-wavelength PDM transmission, based on [33, Fig. 3]. (DAC: Digital-to-analog converter)

hybrid along with a laser beam from the LO. These two beams are mixed in a particular fashion to downconvert the received signal. Analogously, the Y-polarized beam of the received signal enters a different 90° optical hybrid with the other LO laser beam, except it first undergoes polarization rotation to become X-polarized. The outputs from the two hybrids then enter an array of balanced photoreceivers where the in-phase and quadrature components of each polarization are extracted, resulting in four electrical signals. Finally, the signals are sent to an analog-to-digital converter and thereafter to the DSP chain.

2.1 Transmission Impairments

Although this thesis is focused on the compensation of LPN, other impairments cannot be ignored as they will affect the performance of the PNC. This section gives an overview of the main transmission impairments that occur due to physical properties of the fiber-optic channel and imperfections in various hardware components. Impairments that are specific to SDM fibers are not covered in this section.

2.1.1 Additive Noise

The silica core in modern optical fibers through which the lightwave propagates is remarkably transparent. It was introduced in 1979 [34] and was one of the inventions that initiated the rapid progress of fiber-optic communication systems in the coming decades. However, despite its transparency, the silica core exhibits a wavelength-dependent transmission loss, with a minimum loss of approximately 0.2 dB/km for wavelengths at around

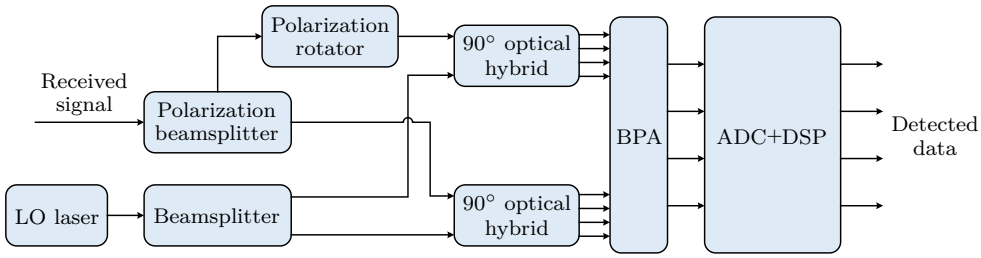

Figure 2.4: Overview of the coherent optical receiver for single-wavelength PDM transmission, based on [33, Fig. 4]. (BPA: Balanced photoreceiver array, ADC: Analog-to-digital converter)

1550 nm. This loss becomes significant in long-haul transmission and has to be compensated; otherwise, the signal will be undetectable at the receiver. Initially, to overcome this problem, optoelectronic regenerators were placed at regular intervals in the optical link that detected and retransmitted the data, but as they had similar costs as typical pairs of endpoint transceivers [35], this solution became expensive and complex for WDM systems. Moreover, regenerators are incompatible with elastic optical networking [36] as they must be configured for a fixed combination of, e.g., baud rate, modulation format, pulse shape, and WDM grid.

In the 1980s, a more economical and flexible way of compensating for the loss was proposed where the optical signal could be amplified simultaneously at multiple wavelengths without the need for detection and retransmission, using an optical amplifier such as the erbium-doped fiber amplifier [6, 7] or the Raman amplifier [37]. However, the amplification is accompanied by a phenomenon called amplified spontaneous emission, which manifests as additive noise in the transmitted signal. This degrades the performance of DSP algorithms and, more importantly, puts a fundamental limitation on the possible transmission reach [38].

2.1.2 Polarization Effects

As previously mentioned, coherent fiber-optic systems exploit the fact that light has two orthogonal polarization states that can be encoded with data independently. This orthogonality is preserved as the signal propagates if the optical fiber has a perfectly cylindrical core. In reality, however, the shape of the core will vary along the fiber due to imperfections in the manufacturing process as well as mechanical and thermal stress, causing the fiber to have a random birefringence[1] [39, Ch. 1.2]. As a consequence, the polarization state of the light rotates randomly during propagation, leading to polarization coupling. Moreover, due to the fiber birefringence, the two polarizations will propagate at different

[1] Birefringence is a property of the fiber material entailing a refractive-index dependence on the polarization of the light.

velocities in the fiber, resulting in a phenomenon called polarization-mode dispersion (PMD) that manifests as pulse broadening [39, Ch. 2.2]. Finally, polarization-dependent loss, typically defined as the ratio between the maximum and minimum polarization-dependent power gains with respect to all possible polarization states [40], is an effect that originates in various optical components [41] and can lower the signal-to-noise ratio (SNR) and orthogonality between the polarizations [42].

2.1.3 Chromatic Dispersion

The optical fiber has a wavelength-dependent refractive index, which originates from a property of the fiber material called chromatic dispersion (CD). Due to this, the different spectral components of the signal travel at different velocities through the fiber [39, Ch. 1.2]. This effect can be regarded as an all-pass filter, i.e., a filter that applies frequency-dependent phase shift to the signal while leaving its amplitude unaffected. It causes a deterministic pulse broadening that increases with the length of the optical link and severely limits the transmission reach of fiber-optic systems if left uncompensated. However, the amount and characteristic of the CD also depend on a dispersion parameter that can be controlled in the fiber design process. As a result, the pulse broadening can be reduced through the use of dispersion-shifted fibers that have minimum dispersion at the carrier wavelength or completely reverted by adding so-called dispersion-compensating fibers to optical links in addition to the standard fibers.

2.1.4 Nonlinearities

In addition to being wavelength dependent, the refractive index of the optical fiber changes in proportion to the light intensity. This phenomenon is called the optical Kerr effect and is the cause of various nonlinear signal effects that occur during propagation, such as self-phase modulation (SPM), cross-phase modulation (XPM), and four-wave mixing (FWM) [39, Ch. 2.6]. These effects degrade the performance of conventional fiber-optic systems if the launch power on the transmitter side is increased beyond a certain point. SPM entails an optical pulse inducing a nonlinear phase shift to itself proportional to its intensity and the optical link length, which also leads to spectral broadening [39, Ch. 4]. XPM occurs during simultaneous transmission of multiple channels, e.g., PDM or WDM signals. Its manifestation is similar to SPM, but the nonlinear phase shift of a pulse is proportional to the light intensity corresponding to copropagating pulses[2] [39, Ch. 7]. FWM is a phenomenon where three copropagating frequency components generate a fourth component with a particular frequency. This leads to interchannel interference and can degrade the performance of WDM systems [30, Ch. 2.3]. Moreover, due to the Kerr effect, light propagating through the fiber produces nonlinear birefringence whose magnitude is dependent on the state of polarization and intensity of

[2]It is worth noting that XPM-induced phase shifts can be approximated as random walks in the case of WDM transmission with ideal distributed Raman amplification [43].

the light. This leads to a self-induced change in the light's state of polarization, referred to as nonlinear polarization rotation [39, Ch. 6.1]. The aforementioned impairments can be partially compensated for in the optical domain [44, 45] or in DSP [46, 47].

Another nonlinear effect pertaining to optical fibers is electrostriction, where light intensity causes the fiber material to become compressed. This effect leads to a process called stimulated Brillouin scattering that puts a limit on the possible launch power [30, Ch. 2.6]. A related process is stimulated Raman scattering, which can negatively affect WDM systems even for modest launch powers. However, it can also be exploited to amplify optical signals, in which case it is known as Raman amplification [37].

2.1.5 Carrier-Frequency Offset and Laser Phase Noise

The coherent receiver in modern systems performs so-called intradyne detection [48], where an LO is mixed with the received signal to extract the in-phase and quadrature components from the polarizations. The LO is tuned to approximately match the frequency of the received carrier wave. However, it is not phase locked to the carrier, which causes a frequency and phase mismatch between the LO and the received signal. This manifests as a linear phase rotation of the received samples after analog-to-digital conversion.

Since coherent systems typically encode information in the amplitude and phase of the light, lasers used for fiber-optic communications should ideally be able to produce a perfect sinusoidal carrier wave. In other words, the optical spectrum of the laser output should be a delta function. In reality, however, this is not the case, as there will be phase fluctuations in the optical field produced by the laser [49, Ch. 7.6]. The fluctuations are statistically independent of each other as they come due to spontaneous emission in the laser. They perturb the carrier phase in a cumulative fashion, giving rise to a process that drifts with time and is called LPN. Each symbol in modulated transmission experiences the accumulation of many such phase fluctuations, which will be approximately Gaussian distributed due to the central limit theorem [50, Ch. 3.1]. As a consequence, LPN is typically modeled as a Gaussian random walk, i.e., a discrete process given by

$$\theta_k = \theta_{k-1} + \Delta\theta_k, \tag{2.1}$$

where θ_k is the LPN at time index k and $\Delta\theta_k$ is a Gaussian random variable with zero mean and variance $2\pi\Delta\nu T_\mathrm{s}$. The parameter T_s is the inverse of the transmission baud rate [50, Ch. 2.5] and $\Delta\nu$ is the combined laser linewidth [51] of the light-source laser at the transmitter and the LO laser at the receiver[3]. Each θ_k manifests as the 2π-periodic rotation $e^{j\theta_k}$ in the complex-valued signal space, and hence, the LPN inherently has a

[3]The phase noise of real lasers does not behave exactly as a random walk [49, Ch. 7.6]. Moreover, due to dispersion, the observed phase noise at the receiver is not simply the sum of phase noise produced by the light-source laser and the LO laser [52]. Nevertheless, (2.1) is the prevailing LPN model used in the literature.

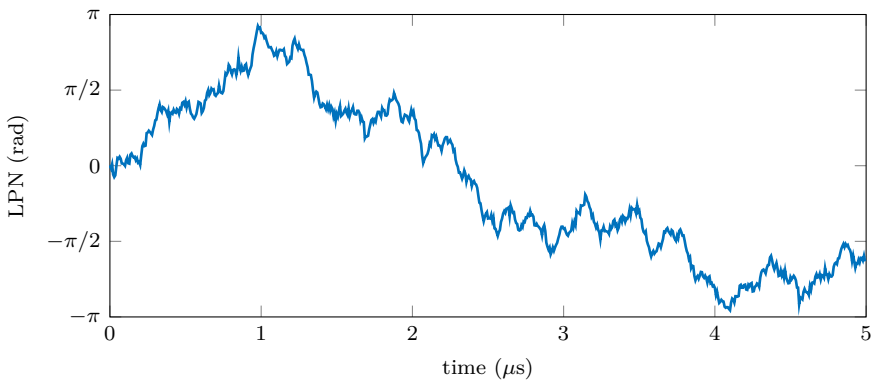

Figure 2.5: A realization of the LPN random-walk model for 28 Gbd transmission and 200 kHz combined laser linewidth.

2π ambiguity. The initial condition θ_0 is typically set to zero or distributed uniformly in the range $[0, 2\pi)$. Fig. 2.5 exemplifies LPN modeled as a random walk for 28 GBd transmission and a combined laser linewidth of 200 kHz.

2.1.6 I/Q Imbalance

As mentioned earlier, in coherent communication systems, information is encoded in the amplitude and phase, i.e., in the orthogonal in-phase and quadrature components of the carrier wave. However, imperfections in the transceiver hardware lead to phase and amplitude errors in the components, causing them to lose orthogonality. This phenomenon is referred to as I/Q imbalance, and its origins on the transmitter side are, e.g., incorrect bias-points settings and imperfect splitting ratio of couplers [53]. On the receiver side, further amplitude and phase errors in the received signal can be caused due to imperfections in the 90° optical hybrids and balanced photodiodes [54].

2.2 Digital Signal Processing in the Coherent Receiver

Fig. 2.6 depicts the basic DSP chain in the coherent receiver required to compensate for the impairments discussed in Section 2.1 and detect the transmitted data. The ordering of the steps in Fig. 2.6 is not unique, and the chain does not include all possible techniques that are performed in the coherent receiver, such as deskewing [55], timing recovery [56], and fiber nonlinearity mitigation [57]. In addition, DSP can be performed on the transmitter side, which is not covered in this thesis. The rest of this section reviews algorithms from the literature to implement all the steps in Fig. 2.6 except for PNC, which will be the focus of Chapter 3. Note that this section does not include specialized multichannel DSP techniques for SDM transmission, but rather focuses on

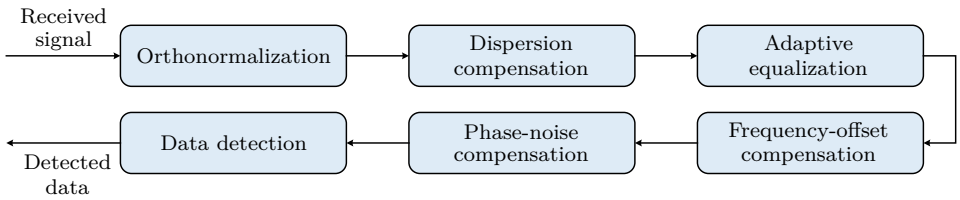

Figure 2.6: A basic DSP chain used in the coherent receiver.

methods that are used in standard SMF transmission. However, these methods can be used on a per-core basis for some SDM systems; indeed, this was the case for the MCF experimental setup used for Paper C, where all DSP stages except for PNC were applied separately on each core.

2.2.1 Orthonormalization

As discussed in Section 2.1.6, I/Q imbalance decreases the orthogonality between the in-phase and quadrature components of a signal. This can be compensated through a process called orthogonalization, and if accompanied with signal normalization to correct for amplitude errors, it is referred to as orthonormalization. Typically, the Gram–Schmidt algorithm is used to achieve this. It was originally developed in the field of mathematics to construct an orthogonal basis from an arbitrary one, and eventually it was utilized to compensate for I/Q imbalance in the context of fiber-optic communications [53]. However, this method increases the impact of quantization noise in one of the signal components. Alternatively, the Löwdin algorithm can be used, which constructs a set of symmetrically orthogonalized components that are closest to the original components in the least mean-squares sense [58]. As a result, the impact of quantization noise is distributed equally in the two components [59]. Other solutions have been proposed specifically for transmission of quadrature phase-shift keying (QPSK) [60–62].

At this stage in the DSP chain, I/Q imbalance that originates in the transmitter cannot be compensated due to the presence of other impairments, such as carrier-frequency offsets and phase noise. Instead, a second orthonormalization step can be performed after PNC.

2.2.2 Dispersion Compensation

CD can be regarded as an all-pass filter with the transfer function [63]

$$G(f) = \exp\left(-j\frac{\pi f^2 \lambda^2 D}{c}\right), \tag{2.2}$$

where c is the speed of light, λ is the carrier wavelength, D is the dispersion parameter, and f is frequency. Since CD affects the two polarizations of the light identically, it can be

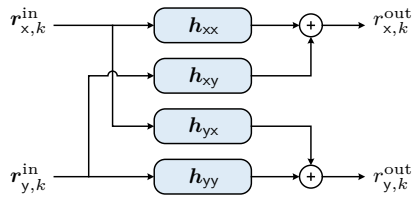

Figure 2.7: Illustration of the adaptive equalizer, entailing four FIR filters and a particular connection between the inputs and the outputs.

compensated through static equalization using identical filters for each polarization with the transfer function $1/G(f)$ [64]. The filtering can be done in the frequency domain, but practical implementations are usually carried out in the time domain using finite impulse response (FIR) or infinite impulse response filters [10, 64–66].

In practical systems, the exact accumulated dispersion is not known even if the dispersion parameters specified for the optical fibers in the link are given. However, multiple blind methods that operate without prior knowledge of the transmitted data have been proposed to estimate the accumulated dispersion [63, 67–69]. Alternatively, pilot-aided methods[4] that utilize signals known to the receiver can be used [70, 71].

2.2.3 Adaptive Equalization

While static equalization may compensate for chromatic dispersion, polarization-dependent impairments such as PMD and polarization rotation/coupling are dynamic phenomena that require adaptive equalization to be undone. Typically, this is carried out at 2 samples per symbol using a multiple-input multiple-output (MIMO) equalizer that consists of four complex-valued FIR filters connecting the inputs and outputs through a so-called butterfly structure [59]. This structure is illustrated in Fig. 2.7, where at each time k, the inputs are windows of received samples around the kth sample, denoted with $\boldsymbol{r}^{\text{in}}_{\text{x},k}$ and $\boldsymbol{r}^{\text{in}}_{\text{y},k}$, and the outputs are equalized samples, denoted with $r^{\text{out}}_{\text{x},k}$ and $r^{\text{out}}_{\text{y},k}$. Moreover, the four FIR filters are denoted as $\boldsymbol{h}_{\text{xx}}$, $\boldsymbol{h}_{\text{xy}}$, $\boldsymbol{h}_{\text{yx}}$, and $\boldsymbol{h}_{\text{yy}}$. The purpose of the equalizer is to reverse the polarization coupling, i.e., demultiplex the polarizations, as well as to mitigate PMD. However, the equalizer also approximates the matched filter and compensates, to some extent, timing errors and residual chromatic dispersion. To accomplish the adaptive equalization, the filter taps are updated in a recursive manner by minimizing a cost function through an update algorithm, such as stochastic gradient descent, until they reach convergence. However, even after convergence, there is no guarantee that the equalizer manages to compensate properly for the aforementioned impairments, and the performance depends on the cost function, the filter tap initialization, and the parameter setting pertaining to the update algorithm.

[4] Blind and pilot-aided methods are also called non-data-aided and data-aided methods, resp.

Several blind equalizers have been proposed in the literature, differing mainly in the cost function used to update the filter taps. The constant modulus algorithm (CMA) [72] is a blind equalizer that relies on the transmitted symbols having constant amplitude, which is the case for PSK modulation. For multimodulus formats such as 16-ary quadrature amplitude modulation (16QAM), the CMA has suboptimal convergence and steady-state performance as the constant-modulus criterion is broken [73]. In this case, other variants are more effective, such as the radially-directed equalizer, also known as the multimodulus algorithm [74], and decision-directed equalizers [75]. Alternatively, a trained equalizer [59] using a sequence of transmitted pilot symbols known to the receiver can be used to achieve equalization with high accuracy. Finally, it is worth noting that the CMA is routinely used for preconvergence of the filter taps, followed by the operation of some of the other aforementioned equalizers, as this is found to improve the overall equalization performance [75].

2.2.4 Frequency-Offset Compensation

While compensating for frequency offsets and phase noise can be done jointly, these steps have traditionally been separated in DSP, and hence, the linear phase rotations caused by frequency offsets in the receiver are mitigated prior to the PNC. Numerous blind algorithms have been proposed for frequency-offset estimation. A differential phase-based method can be used where the maximum likelihood estimate of the frequency offset is obtained [76]. A similar method was proposed in [77], but it performs the estimation in a recursive manner. Spectral methods can also be used, where the received samples are preprocessed (typically raised to the fourth power) and then Fourier transformed, which allows searching for a peak in the spectrum corresponding to the frequency offset [78]. An iterative method based on this concept was proposed in [79], improving upon the estimation accuracy and effectiveness for higher-order QAM. Multiple other blind and pilot-aided algorithms exist and were reviewed in [78].

2.2.5 Data Detection

After all impairments have been compensated, data detection is performed, which is the process of recovering the data-bit sequence that was conveyed over the optical channel. In general, reliability demands are extremely stringent for fiber-optic communication systems, where a bit error rate (BER) of down to 10^{-15} is required [80]. Particularly for long-haul systems with high spectral efficiencies, the only way to meet these demands is through the utilization of error correcting codes, typically referred to as forward error correction (FEC) in the context of fiber-optic communications. Common FEC codes include low-density parity-check [81] or Reed–Solomon [82] codes. Moreover, depending on the type of code, either soft-decision or hard-decision decoding can be performed, where the latter has less computational complexity at the cost of degraded performance compared to the former [83]. The decoder inputs are based on the likelihood functions

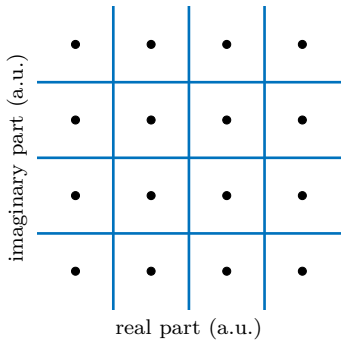

Figure 2.8: A decision-region illustration of the minimum-Euclidean-distance symbol detector for 16QAM in the case of equiprobable symbols, where the black dots and blue lines correspond to constellation points and edges of the decision regions, resp.

of the transmitted symbols, which are typically computed under the assumption that all data-bit sequences are equiprobable and that the only remaining signal impairment is additive white Gaussian noise (AWGN). In that case, the likelihood functions are computed from the Euclidean distance between the received samples and the constellation points.

For uncoded transmission, data detection is simpler and is typically carried out through symbol detection followed by symbol-to-bit mapping. The maximum *a posteriori* (MAP) symbol detector is optimal in the sense that it yields minimum symbol error rate. For the AWGN channel and equiprobable symbols, this detector operates on a symbol-by-symbol basis and detects each symbol by finding the constellation point closest to the received sample in terms of Euclidean distance [50, Ch. 3.4]. This can be geometrically interpreted as the use of decision regions in the complex-valued signal space, depicted in Fig. 2.8 for 16QAM. However, performing symbol detection and symbol-to-bit mapping to yield the detected data bits is in general suboptimal in terms of minimizing the BER [84].

If minimum BER is the objective, the MAP bit detector should be used. It has been derived or approximated for various channel models [85, 86], and in Paper A, we approximate it for coded multichannel transmission in the presence of arbitrarily correlated phase noise.

CHAPTER 3

Phase-Noise Compensation

The presence of LPN[1] necessitates the use of PNC prior to data detection. The problem of PNC has been studied for a long time in the context of fiber-optic and wireless communication systems[2] and continues to be an active area of research. This is owing to the increased focus on higher-order QAM since these modulation formats allow for an increased spectral efficiency but come with a higher sensitivity to transmission impairments, in particular LPN.

One way to design PNC algorithms is by applying detection-and-estimation theory to an appropriate system model. Therefore, this chapter gives a brief explanation of optimal bit detection for a single channel in the presence of AWGN and phase noise, which serves as a preliminary to Paper A where this problem is addressed in a multichannel scenario. Thereafter, an overview will be given of various blind and pilot-aided algorithms found in the literature for single-channel PNC based on heuristic arguments or designed using theoretical frameworks. Moreover, as Papers B–C are centered on PNC for SDM systems, different PNC strategies for multichannel transmission in the presence of phase noise are reviewed.

[1] Nonlinear phase noise can also require the use of PNC techniques [43]. However, this thesis will focus on the compensation of LPN.

[2] Analogous to LPN in fiber-optic systems is oscillator phase noise in wireless systems.

3.1 Optimal Detection in the Presence of Phase Noise

MAP bit detection is an optimal strategy in the sense that it minimizes the resulting BER [87, Ch. 1.4]. It performs detection on a bit-by-bit basis by computing

$$\hat{b} = \underset{b\in\{0,1\}}{\operatorname{argmax}} P(b|\boldsymbol{r}), \tag{3.1}$$

where b is the information bit, $\boldsymbol{r}$ comprises all received samples, and $P(b|\boldsymbol{r})$ is the *a posteriori* PMF of b. For trivial scenarios such as uncoded transmission over the AWGN channel, the PMF in (3.1) is mathematically tractable. However, for more complicated models, obtaining $P(b|\boldsymbol{r})$ is nontrivial.

Consider a block of K information bits, $\boldsymbol{b} = [b_1, \ldots, b_K]$, mapped to a block of N symbols, $\boldsymbol{s} = [s_1, \ldots, s_N]$, through a deterministic function that represents the FEC code and modulation format, and transmitted over a single channel in the presence of AWGN and LPN. A common discrete-time complex baseband model for this scenario is

$$r_k = s_k e^{j\theta_k} + n_k, \tag{3.2}$$

for $k = 1, \ldots, N$, where r_k, s_k, θ_k, and n_k are the received sample, transmitted symbol, phase noise, and AWGN, resp. Moreover, $\boldsymbol{r} = [r_1, \ldots, r_N]$ contains all received samples, and $\boldsymbol{s}$, $\boldsymbol{\theta}$, and $\boldsymbol{n}$ are defined similarly. For the model in (3.2), $P(b_l|\boldsymbol{r})$ is hard to compute due to the presence of an FEC code and phase noise, but it can be obtained by marginalizing the joint distribution of all the system parameters, $p(\boldsymbol{b}, \boldsymbol{s}, \boldsymbol{\theta}|\boldsymbol{r})$, over all $\boldsymbol{s}$, $\boldsymbol{\theta}$, and $\boldsymbol{b}$ except for b_l [85]. Carrying out this marginalization exactly yields a MAP bit detection algorithm that jointly performs PNC and decoding. It is interesting to note that it treats the phase noise as a nuisance parameter [88, Ch. 10.7], i.e., $\boldsymbol{\theta}$ is simply integrated out, and as a consequence, explicit phase-noise estimates are not needed.

Solving the marginalization in closed form is hard in general, and numerical evaluation is impractical due to the presence of integrals. However, several Bayesian inference techniques and frameworks can be used to carry out the marginalization approximately but efficiently. Examples include the expectation–maximization [89] algorithm, variational Bayesian (VB) inference [90], factor graphs (FGs) and the sum–product algorithm (SPA) [91], and various sequential Monte Carlo methods [92]. Two of these examples, namely the FG/SPA and VB frameworks, are used to develop the proposed algorithms in Paper A. The algorithms do not obtain explicit phase-noise estimates, but instead, the *a posteriori* PDFs are estimated through extended Kalman smoothing [93, Ch. 8.2] and used when computing the decoder inputs.

3.2 Single-Channel Processing

3.2.1 Blind Algorithms

As previously mentioned, pilot symbols do not carry any data and thus reduce the overall spectral efficiency of the system. To avoid the reduction in spectral efficiency, most PNC algorithms in fiber-optic communications have traditionally been blind. Moreover, to simplify implementations in hardware, algorithms are often designed to operate in a feedforward manner, i.e., without containing any feedback loops [94].

Although blind algorithms have no *a priori* knowledge of the transmitted symbols, the structure of certain modulation formats can be exploited to allow estimating the phase noise. As an example, M-PSK comprises M equispaced constellation points on a circle in the complex plane. When symbols corresponding to this modulation are raised to the Mth power, the modulation is removed and the phase noise can be estimated in a range of length $2\pi/M$. The phase-noise estimates are processed and then used to derotate the signal, which mitigates the phase noise. To illustrate the concept, Fig. 3.1 shows the general steps used by these techniques for QPSK. The Viterbi–Viterbi algorithm [95] and similar feedforward methods [96] are based on this concept and work effectively for QPSK. However, for higher-order QAM, these methods work suboptimally as the constellation points generally do not have equispaced phases. Among the most widely-used blind algorithms in fiber-optic communications for QAM is the BPS [94], a feedforward algorithm that yields good performance in terms of laser linewidth tolerance but has a high computational complexity for higher-order formats. Several BPS variants have been proposed that reduce the required computational complexity while maintaining the performance of the original method [97–99]. Furthermore, in the case of 16QAM, PNC based on QPSK partitioning [100] or decision-directed least-mean square filtering [101] has been proposed.

An inherent problem with blind algorithms is ambiguity in the estimated phase noise. Due to the rotational symmetry that is associated with most modulation formats, the phase noise can only be estimated unambiguously in a limited range. As a consequence, the phase-noise estimates need to be unwrapped, which is done recursively and thus adds a feedback mechanism to the system. This can lead to cycle slips for low SNRs or sufficient levels of phase noise, which in turn cause bursts of errors [96]. Multiple solutions to this have been proposed, e.g., differential encoding [102], which increases the BER in the absence of cycle slips [96], and the use of pilots for framing information [103] or cycle-slips mitigation [104].

3.2.2 Pilot-Aided Algorithms

An alternative to blind estimation is to use pilot-aided algorithms that are independent of the modulation and yield unambiguous estimates of the phase noise. Pilot-aided algorithms have been researched extensively, particularly in the context of wireless com-

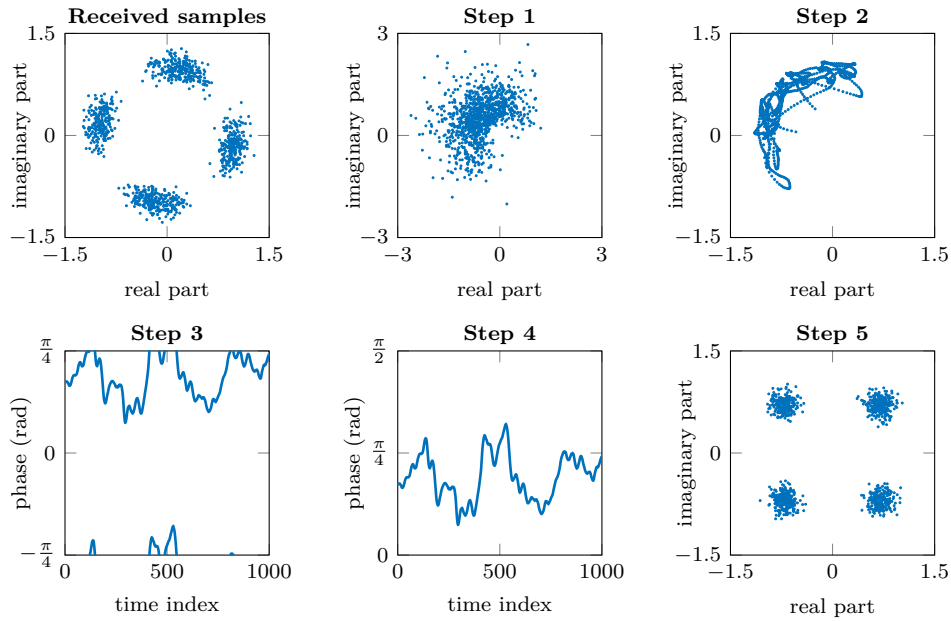

Figure 3.1: Illustration of PNC using the Mth-power method for QPSK. Step 1: Raise the received complex samples to the 4th power to remove the phase modulation. Step 2: Filter the 4th-power samples to mitigate distortions from the AWGN. Step 3: Take the angle of the filtered samples and divide by four, which yields wrapped phase-noise estimates in a range of length $\pi/2$. Step 4: Unwrap the estimates. Step 5: Derotate the received samples to obtain phase-noise compensated samples.

munications. However, they have also gained significant traction in the optical literature recently[3] due to their high performance, which becomes beneficial for transmission of higher-order QAM.

Many examples can be found where pilot-aided algorithms are derived using probabilistic inference frameworks that approximate optimal detection in the presence of phase noise, exploiting the statistical structure of the system model. In [43], an algorithm that compensates for LPN and nonlinear phase noise for WDM transmission with ideal distributed Raman amplification is proposed using probabilistic arguments. Moreover, considering coded transmission in the presence of phase noise, [86, 110] use the FG and SPA framework [91] to derive algorithms that perform iterative phase-noise estimation and decoding. A similar scenario is considered in [111] where the VB framework [90] is used to derive an iterative algorithm. In [112], the algorithm proposed in [86, Sec. IV-B] is extended to perform joint-polarization PNC for PDM transmission. A method based on Kalman filtering [113] and the expectation–maximization [89] algorithm is proposed

[3]Pilot rates used in recent literature have typically been 3% or less [105–109].

in [114] and experimentally validated. Finally, a literature review of various symbol detectors for transmission in the presence of phase noise is given in [115].

3.3 Multichannel Processing

Multichannel transmission plays an important role in fiber-optic communications and has existed for decades in the form of WDM systems, where multiple carriers of different wavelengths are transmitted simultaneously over the same spatial channel. Furthermore, thanks to the coherent receiver and DSP, PDM transmission can be realized where the two polarizations on each carrier are used to transmit independent data. More recently, SDM transmission has gained significant research interest, in which multiple spatial channels are transmitted simultaneously at the same wavelength. Multichannel transmission is also an integral part of wireless MIMO communication systems.

Certain transmission impairments, in particular LPN, are highly correlated across the multiplexed channels in various multichannel transmission scenarios, e.g., SDM systems using specific types of fibers where all spatial channels share the light source and LO lasers [116, 117], WDM systems using frequency combs to act as a light source and LO for all wavelength channels [118], and electrically generated subcarrier systems [119]. The phase-noise correlation can be exploited to reduce computational complexity in DSP, e.g., through specialized transmission techniques such as self-homodyne detection [120, 121], where a pilot tone, i.e., an unmodulated carrier, is transmitted in one channel and used as an LO at the receiver, thereby canceling the LPN that originates on the transmitter side. Moreover, DSP-based methods such as master–slave processing [116] can be used, where phase-noise estimation is performed on a single selected channel and the resulting estimates are used to compensate for the phase noise in all channels. These methods rely on the phase noise being identical across all channels, which is typically not the case in reality due to system characteristics/imperfections and environmental factors [122]; hence, their performance may suffer.

Alternatively to reducing complexity, performance can be improved in terms of linewidth tolerance by exploiting the phase-noise correlation through joint-channel processing, which entails estimating the phase noise collectively across all the channels. The improved tolerance can be used to increase power/spectral efficiency, relax laser requirements, or extend transmission reach, at the cost of added computational complexity. The rest of this section discusses joint-channel PNC for perfect and partial phase-noise correlation.

3.3.1 Perfect Phase-Noise Correlation

Ideally, the phase noise is perfectly correlated across the channels, in which case joint-channel processing yields the biggest benefits. To quantify the gains, consider the following example pertaining to a system model describing transmission over D parallel

channels, each containing N independent symbols. Assuming identical phase noise in all channels, the discrete-time observation at time k is

$$\mathbf{r}_k = \mathbf{s}_k e^{j\theta_k} + \mathbf{n}_k, \tag{3.3}$$

for $k = 1, \ldots, N$, where $\mathbf{s}_k = [s_{1,k}, \ldots, s_{D,k}]^{\mathrm{T}}$ denotes a vector of independent symbols at time k. Each data symbol is modeled as a random variable, drawn uniformly from a set of constellation points, whereas pilot symbols take on a complex value, known to both the transmitter and the receiver. The average symbol energy of the constellation is E_{s}. Furthermore, $\mathbf{n}_k$ denotes a vector containing samples of complex AWGN with variance N_0 and θ_k is LPN, modeled as a random walk, i.e., $\theta_k = \theta_{k-1} + \Delta\theta_k$, where $\Delta\theta_k$ is a Gaussian random variable with variance $\sigma^2 = 2\pi\Delta\nu T_{\mathrm{s}}$, for a combined laser linewidth $\Delta\nu$ and symbol rate $1/T_{\mathrm{s}}$.

This ideal model allows extending single-channel PNC algorithms in a trivial manner such that they essentially perform estimate averaging across the channels. As an example, the BPS [94] can be extended as follows. Starting with an initial estimate $\hat{\theta}_0$ (e.g., obtained from a pilot sequence), the algorithm sequentially determines estimates of the phase noise. At time k, the vector $\mathbf{r}_k$ is rotated by B test phases, $\phi_b = \hat{\theta}_{k-1} + \pi b/(2B)$, $b = -B/2+1, \ldots, B/2$. Denoting the corresponding hard decision after rotation by $\hat{\mathbf{x}}_{k,b}$, the most probable test phase is then found by solving

$$b_k^* = \arg\min_b \sum_{n=k-L/2}^{k+L/2} \|\hat{\mathbf{x}}_{n,b} - \mathbf{r}_n \exp(j\phi_b)\|^2, \tag{3.4}$$

where L determines an observation window in the time domain[4]. Finally, the estimate of the total phase at time k is given by $\hat{\theta}_k = \hat{\theta}_{k-1} + \pi b_k^*/(2B)$, after which the algorithm moves on to time $k+1$. The benefit of using multiple channels is the possibility to reduce L by averaging in the channel domain, rather than in the time domain, thus enabling faster tracking [94].

To compare the performance difference between per-channel and joint-channel processing, the extended BPS is assessed through Monte Carlo simulations of uncoded 256QAM transmission over $D = \{2, 6, 20\}$ channels. The symbol rate and laser linewidth are fixed at 28 Gbaud and 200 kHz, resp. For each BER estimate, blocks of $N = 10^4$ symbols per channel are transmitted repeatedly until the total number of bit errors reaches at least 1000. To quantify the penalty due to phase noise, the required SNR per information bit for a target BER of 10^{-2} is computed. This SNR is then compared to the theoretically required SNR to attain a BER of 10^{-2} for the AWGN channel in the absence of phase noise, which is approximately 16.4 dB assuming Gray-mapped constellations [123]. Fig. 3.2 depicts the performance of the extended BPS with $B = 64$. Comparing per-channel and joint-channel processing of 20 channels, the optimal L that yields the smallest SNR

[4] The quantities inside the summation in (3.4) are zero padded such that the observation window is valid for all $k = 1, \ldots, N$.

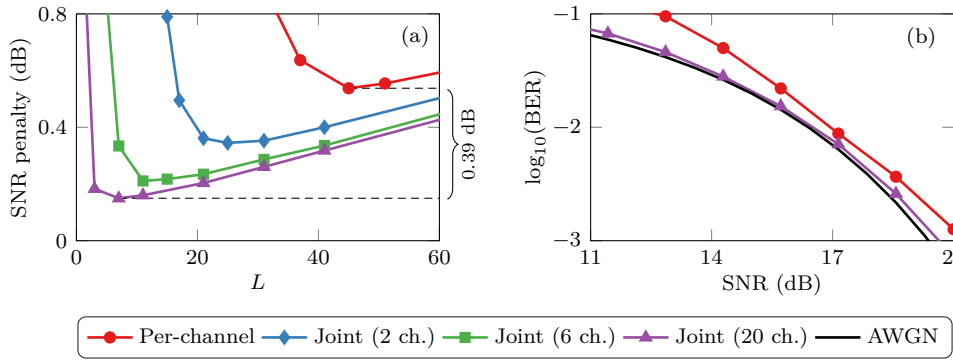

Figure 3.2: (a) SNR penalty versus L at a fixed BER of 10^{-2} and (b) BER versus SNR for a fixed L.

penalty at a BER of 10^{-2} reduces from 45 to 7. Moreover, the minimum SNR penalty attained at the optimal L decreases for joint-channel processing as the number of channels grows, as can be seen in Fig. 3.2 (a). The difference in the minimum SNR penalty between per-channel and joint-channel processing of 20 channels is approximately 0.39 dB, with only 0.15 dB remaining to the required SNR for the AWGN channel through joint-channel processing. Fig. 3.2 (b) shows the BER of per-channel and joint-channel processing of 20 channels, with L chosen for each curve such that the SNR penalty at a BER of 10^{-2} is minimized. As the SNR decreases, the performance of per-channel processing degrades severely due to cycle slips, while joint-channel processing maintains a low SNR penalty for all simulated SNRs.

3.3.2 Partial Phase-Noise Correlation

As already mentioned, no system gives rise to perfectly correlated phase noise across all channels. Instead, the phase noise will typically contain a dominant component corresponding to the LPN, in addition to channel-specific phase drifts. As a result, more sophisticated system models and algorithms are needed to properly exploit the phase-noise correlation. Joint-channel PNC has been studied for more realistic models in the context of wireless communications [124–126], for WDM fiber-optic systems using frequency combs [105], and for a general optical multichannel system in Paper A. Moreover, Paper C introduces a multichannel phase-noise model that describes partially-correlated phase noise for transmission using a particular type of MCF. Using one of the algorithms from Paper A, an extensive study on the performance gains through joint-channel PNC is done based on simulations and experiments.

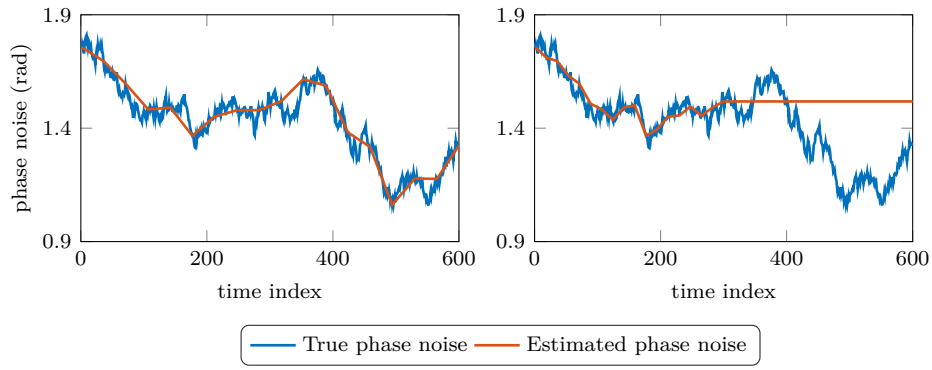

Figure 3.3: True and estimated phase noise where in (a), pilots are placed at every other time index, and in (b), all the pilots are placed in the first half of the symbol block.

3.3.3 Pilot-Symbol Placements

In general, the placements of pilot symbols can heavily affect the performance of pilot-aided PNC algorithms. Fig. 3.3 demonstrates this where the true and estimated phase noise[5] are plotted for two different pilot-symbol arrangements with 3% overall pilot rate; in Fig. 3.3 (a), the pilot symbols are equispaced throughout the symbol block whereas in Fig. 3.3 (b), the first and seconds halves of the symbol block have 6% and 0% pilot rates, resp. Paper B studies this problem in a multichannel setting, where several two-dimensional arrangements (across the time and channel domains) of pilot symbols are compared in terms of the resulting phase-noise tolerance for different correlations and levels of phase noise.

[5] The phase-noise estimates are obtained using the proposed algorithm in [86, Sec. IV-B] without decoder feedback.

CHAPTER 4

Fiber Designs for Space-Division Multiplexing

As discussed in Chapter 1, SDM has received significant attention lately in response to the ever-increasing Internet traffic growth. The goal of SDM is to increase the capacity of optical links by transmitting multiple spatial channels in parallel, while keeping the associated cost down through the integration of system components and the use of specialized fibers. The rest of this chapter will briefly review different fiber designs that can be used to implement SDM transmission. The cross sections of the considered fibers are illustrated in Fig. 4.1.

4.1 Bundles of Single-Mode Fibers

The most straightforward approach to realize SDM transmission is to transmit parallel spatial channels over a bundle of multiple SMFs, illustrated in Fig. 4.1 (a). It is simple to implement but has limited potential when it comes to component integration and dense packing of spatial channels [12]. As a consequence, it is not a viable strategy to reduce the cost of upscaling optical networks.

4.2 Multicore Fibers

Fibers where the cladding contains several single-mode cores are called MCFs. The first fabrication of an MCF was reported in the 1970s [29], but it gained limited traction until recently when interest in SDM was revitalized. Today, several types of MCFs are being researched and fabricated worldwide.

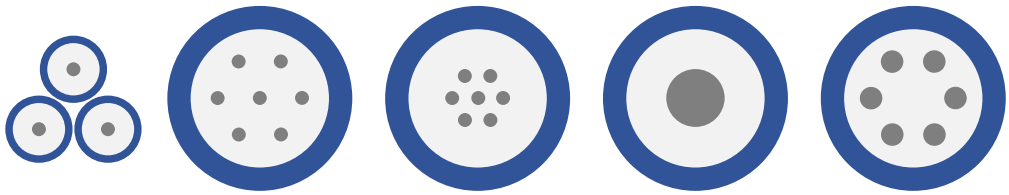

Figure 4.1: Fiber designs that can be used for SDM transmission, where (a) is a fiber bundle, (b)–(c) are uncoupled and strongly-coupled MCFs, resp., (d) is an MMF, and (e) is a multicore–multimode fiber.

Uncoupled-core MCFs, illustrated in Fig. 4.1 (b), are designed such that the intercore crosstalk, which is mainly governed by the core spacing, is minimized. This results in essentially independent parallel spatial channels that are easily separated at the receiver without the need for high-complexity equalization. A further distinction can be made for uncoupled-core MCFs. In homogeneous fibers, all the cores have identical radii and refractive indices, and hence, the same propagation characteristics. As such, the signals propagating through the cores arrive almost simultaneously[1] at the receiver, which can simplify effective optical switching [116] as well as various joint DSP and transmission techniques such as self-homodyne detection [120], PNC [Paper C], and multidimensional modulation [128]. Furthermore, homogeneous MCFs were used in the experiments that hold the current records for the throughput of any MCF (2.15 Pb/s) [129] and the throughput–distance product of any optical fiber (4.59 Eb $\cdot$ km/s) [130].

In contrast to the homogeneous variant, the cores in heterogeneous fibers have different radii and refractive indices, which reduces the intercore crosstalk and thus enables a higher number of cores for a fixed core diameter [131]. This is evident from the standing demonstration records for the maximum number of cores, which are 22 and 32 for homogeneous [129] and heterogeneous [132] MCFs, resp., for similar cladding diameters. However, possible disadvantages associated with heterogeneous MCFs are, e.g., higher manufacturing costs and splice losses compared to homogeneous MCFs. Moreover, the signals experience core-dependent velocities, causing propagation delays between the cores, a phenomenon referred to as intercore skew. This can necessitate a more complicated joint-channel DSP than what is required for homogeneous MCFs. Particularly in the case of transmission where a light source is shared for all the cores, the skew decorrelates the phase noise across the cores and reduces the benefits of joint-channel PNC.

Coupled-core MCFs, illustrated in Fig. 4.1 (c), are designed to have high amounts of intercore crosstalk. This is achieved by spacing the cores closely, which enables a

[1] Due to environmental factors and system imperfections, the signals will typically not arrive at exactly the same time [127].

denser packing of spatial channels compared to uncoupled-core MCFs. However, the presence of core coupling and intercore skew results in signal dispersion and mixing during propagation through the cores, which requires high-complexity equalization at the receiver, analogous to polarization demultiplexing in the case of PDM transmission. Hence, coupled-core MCFs are typically engineered to minimize the dispersion in order to reduce the required equalization complexity [133].

4.3 Multimode Fibers

The concept of MMFs was originally proposed decades ago, with the first fabrication reported in the 1970s [134]. In contrast to MCFs, MMFs have only one core within the cladding as illustrated in Fig. 4.1 (d), but the core diameter is wide enough to allow for the propagation of multiple modes. MMFs have traditionally been used for noncoherent transmission in cost-constrained applications such as short-haul links in optical networks, but for coherent SDM transmission, high-complexity equalization is necessary at the receiver due to mode coupling and modal dispersion. However, it has been shown that MMFs can simplify the upscaling of optical-network switches [135] and reduce nonlinearities [136]. As a result, MMFs have been studied extensively in recent years for SDM applications, in which case they are often referred to as few-mode fibers since they are designed to support only a limited number of modes, with 15 being the highest number of modes in successful transmission thus far [137].

4.4 Multicore–Multimode Fibers

In addition to plain MCFs and MMFs, mixtures of the two kinds have also been fabricated and studied, where multiple multimode cores are located within the same cladding as depicted in Fig. 4.1 (e). This type of fiber holds the record for the highest number of spatial channels supported by a single fiber, where PDM transmission of 114 spatial channels through a 6-mode 19-core fiber was demonstrated in [138].

CHAPTER 5

Contributions

This chapter summarizes the contributions of each appended publication and lays out possible directions for future work based on the topics in this thesis.

5.1 Paper A

"Iterative detection and phase-noise compensation for coded multichannel optical transmission"

In this paper, motivated by the fact that various multichannel fiber-optic systems have highly correlated phase noise across the channels, we address the problem of optimal bit detection for multichannel coded optical transmission in the presence of arbitrarily-correlated phase noise. We propose two pilot-aided approximations to the optimal bit detector using different frameworks that can be utilized to simplify Bayesian inference problems. Moreover, the phase noise is modeled as a multidimensional Gaussian random walk, and hence, we effectively estimate it jointly for all channels using an extended Kalman smoother. We further show that the system-model linearization imposed by the extended Kalman smoother does not degrade the performance for practical laser linewidths and symbol rates. Finally, the proposed algorithms are compared to each other and to the BPS algorithm in terms of phase-noise tolerance. Simulation results show that the proposed algorithms perform similarly to each other but significantly outperform the BPS algorithm.

Contributions: AFA developed the algorithms, performed all simulations, and wrote

the paper. EA and HW contributed to the derivations and simulations. All authors reviewed and revised the paper.

Context: Sections 3.1 and 3.3.

5.2 Paper B

"Pilot distributions for phase tracking in space-division multiplexed systems"

In this paper, we study the effect of pilot-symbol arrangements on pilot-aided, joint-channel PNC for SDM transmission in the presence of correlated phase noise, using one of the proposed algorithms from Paper A. Several two-dimensional pilot-symbol arrangements are compared in terms of the resulting algorithm phase-noise tolerance for different laser linewidths and levels of phase-noise correlation. Simulation results show that the pilot-symbol arrangement can significantly affect the algorithm performance. More specifically, it is found that placing the pilots identically in all channels or putting all pilots in a single channel are suboptimal strategies.

Contributions: AFA formulated the problem, introduced the pilot-symbol arrangements, performed the simulations, and wrote the paper. EA helped with the problem formulation. All authors reviewed and revised the paper.

Context: Section 3.3.

5.3 Paper C

"On the performance of joint-channel carrier-phase estimation in space-division multiplexed multicore fiber transmission"

In this paper, we investigate the benefits of joint-channel PNC for SDM transmission through an uncoupled-core, homogeneous, single-mode MCF, where the light source and LO lasers are shared for all cores. To that end, we propose a multichannel system model that describes a common LPN in addition to core- and polarization-specific phase drifts. It is further shown that the phase noise described by the model can be regarded as a multidimensional random walk. Thereafter, one of the proposed algorithms from Paper A is used to implement two PNC strategies, namely per-channel and joint-channel processing. The strategies are compared in terms of phase-noise tolerance using simulations and experimental data, and the performance improvements through joint-channel PNC are translated to gains in power or spectral efficiency, relaxed hardware requirements, and increased transmission reach. Furthermore, strong agreements are observed between experimental and simulation results, which serve to validate the system model.

Contributions: AFA formulated the problem, performed the simulations, processed the experimental data, and wrote the paper. EA, MK, and HW assisted with the problem

formulation. BP, RSL, and GR provided the experimental data. In addition, RSL assisted with the signal processing. All authors reviewed and revised the paper.

Context: Sections 3.3 and 4.2.

5.4 Future Work

In the experimental data used in Paper C, the intercore phase drifts came mostly from core-specific residual frequency offsets due to the specific setup that was used. The random-walk assumption in the phase-noise model used in Paper C is inaccurate in this case, but the model could be extended to include biased random walks that account for the linear drifts caused by frequency offsets. Using this extended model, the algorithms proposed in Paper A could also be extended to account for these random-walk biases, which would allow for a more effective PNC in the presence of residual frequency offsets. Moreover, I/Q imbalance from the transmitter side was an unforeseen issue when using the algorithm from Paper A to perform PNC and data detection for the experimental data. This is owing to the algorithm operating based on the assumption that PNC is the last DSP step prior to data detection, and hence, it had to be slightly modified such that orthonormalization was performed before detecting the data. It is not clear if this modification caused performance degradations to the algorithm. Hence, including transmitted-based I/Q imbalance in the phase-noise model and developing an algorithm that properly takes this impairment into account could be useful to clarify this doubt.

Intercore skew is hard to avoid completely, even for homogeneous MCF systems, and can degrade the performance of PNC methods that rely on the phase-noise correlation. The effect of intercore skew has been studied in the context of self-homodyne detection for SDM transmission [127] and it could be useful to do an analogous study for the algorithms in Paper A.

The algorithms proposed in Paper A could be applied to study the benefits of joint PNC for different multichannel systems with correlated phase noise, e.g., WDM-based systems using frequency combs as light sources as LOs. However, the characteristics of the interchannel phase drifts in these systems are likely to be different from the scenario studied in Paper C, and hence, a new phase-noise model would be required. Another interesting direction is to investigate joint-channel PNC for other SDM transmission scenarios, for example systems using coupled-core MCFs, MMFs, or bundles of SMFs. The characteristics of these alternatives are fairly different from the system considered in Paper C, and it would therefore be interesting to study the benefits of joint-channel PNC for those scenarios.

Bibliography

[1] D. Crowley, P. Urquhart, and P. Heyer, *Communication in History: Stone-Age Symbols to Social Media*, 7th ed. New York, NY, USA: Routledge, 2018.

[2] CISCO, "The zettabyte era: Trends and analysis, white pages," https://www.cisco.com/c/en/us/solutions/collateral/service-provider/visual-networking-index-vni/vni-hyperconnectivity-wp.pdf, Tech. Rep., Jun. 2017, accessed: 2018-08-10.

[3] T. H. Maiman, "Stimulated optical radiation in ruby," *Nature*, vol. 187, pp. 493–494, Aug. 1960.

[4] K. C. Kao and G. A. Hockham, "Dielectric-fibre surface waveguides for optical frequencies," *Proceedings of the Institution of Electrical Engineers*, vol. 113, no. 7, pp. 1151–1158, Jul. 1966.

[5] F. P. Kapron, D. B. Keck, and R. D. Maurer, "Radiation losses in glass optical waveguides," *APL Applied Physics Letters*, vol. 17, no. 10, pp. 423–425, Nov. 1970.

[6] R. J. Mears, L. Reekie, I. M. Jauncey, and D. N. Payne, "Low-noise erbium-doped fibre amplifier operating at 1.54μm," *IET Electronic Letters*, vol. 23, no. 19, pp. 1026–1028, Sep. 1987.

[7] E. Desurvire, J. R. Simpson, and P. C. Becker, "High-gain erbium-doped traveling-wave fiber amplifier," *Optics Letters*, vol. 12, no. 11, pp. 888–890, Nov. 1987.

[8] W. J. Tomlinson, "Wavelength multiplexing in multimode optical fibers," *Applied Optics*, vol. 16, no. 8, pp. 2180–2194, Aug. 1977.

[9] R. A. Linke and A. H. Gnauck, "High-capacity coherent lightwave systems," *Journal of Lightwave Technology*, vol. 6, no. 11, pp. 1750–1769, Nov. 1988.

[10] M. G. Taylor, "Coherent detection method using DSP for demodulation of signal and subsequent equalization of propagation impairments," *IEEE Photonics Technology Letters*, vol. 16, no. 2, pp. 674–676, Feb. 2004.

[11] H. Sun, K.-T. Wu, and K. Roberts, "Real-time measurements of a 40 Gb/s coherent system," *Optics Express*, vol. 16, no. 2, pp. 873–879, Jan. 2008.

[12] E. Agrell, M. Karlsson, A. R. Chraplyvy, D. J. Richardson, P. M. Krummrich, P. Winzer, K. Roberts, J. K. Fischer, S. J. Savory, B. J. Eggleton, M. Secondini, F. R. Kschischang, A. Lord, J. Prat, I. Tomkos, J. E. Bowers, S. Srinivasan, M. Brandt-Pearce, and N. Gisin, "Roadmap of optical communications," *Journal of Optics*, vol. 18, no. 6, pp. 1–40, May 2016.

[13] C. E. Shannon, "A mathematical theory of communication," *The Bell System Technical Journal*, vol. 27, no. 3, pp. 379–423, Jul. 1948.

[14] R. Kashyap and K. J. Blow, "Observation of catastrophic self-propelled self-focusing in optical fibres," *IET Electronic Letters*, vol. 24, no. 1, pp. 47–49, Jan. 1988.

[15] R.-J. Essiambre, G. Kramer, P. J. Winzer, G. J. Foschini, and B. Goebel, "Capacity limits of optical fiber networks," *Journal of Lightwave Technology*, vol. 28, no. 4, pp. 662–701, Feb. 2010.

[16] H. Masuda, E. Yamazaki, A. Sano, T. Yoshimatsu, T. Kobayashi, E. Yoshida, Y. Miyamoto, S. Matsuoka, Y. Takatori, M. Mizoguchi, K. Okada, K. Hagimoto, T. Yamada, and S. Kamei, "13.5-Tb/s (135×111-Gb/s/ch) no-guard-interval coherent OFDM transmission over 6,248 km using SNR maximized second-order DRA in the extended L-band," in *Proc. Optical Fiber Communication Conference (OFC)*, Mar. 2009, p. PDPB5.

[17] M. Mazurczyk, D. G. Foursa, H. G. Batshon, H. Zhang, C. R. Davidson, J.-X. Cai, A. Pilipetskii, G. Mohs, and N. S. Bergano, "30 Tb/s transmission over 6,630 km using 16QAM signals at 6.1 bits/s/Hz spectral efficiency," in *Proc. European Conference on Optical Communication (ECOC)*, Sep. 2012, p. Th.3.C.2.

[18] D. G. Foursa, H. G. Batshon, H. Zhang, M. Mazurczyk, J.-X. Cai, O. Sinkin, A. Pilipetskii, G. Mohs, and N. S. Bergano, "44.1 Tb/s transmission over 9,100 km using coded modulation based on 16QAM signals at 4.9 bits/s/Hz spectral efficiency," in *Proc. European Conference on Optical Communication (ECOC)*, Sep. 2013, p. PD3.E.1.

[19] J.-X. Cai, Y. Sun, H. Zhang, H. G. Batshon, M. V. Mazurczyk, O. V. Sinkin, D. G. Foursa, and A. Pilipetskii, "49.3 Tb/s transmission over 9100 km using C+L EDFA and 54 Tb/s transmission over 9150 km using hybrid-Raman EDFA," *Journal of Lightwave Technology*, vol. 33, no. 13, pp. 2724–2734, Jul. 2015.

[20] A. Ghazisaeidi, I. F. de Jauregui Ruiz, R. Rios-Müller, L. Schmalen, P. Tran, P. Brindel, A. C. Meseguer, Q. Hu, F. Buchali, G. Charlet, and J. Renaudier, "Advanced C+L-band transoceanic transmission systems based on probabilistically shaped PDM-64QAM," *Journal of Lightwave Technology*, vol. 35, no. 7, pp. 1291–1299, Apr. 2017.

[21] J.-X. Cai, H. G. Batshon, M. V. Mazurczyk, O. V. Sinkin, D. Wang, M. Paskov, W. W. Patterson, C. R. Davidson, P. C. Corbett, G. M. Wolter, T. E. Hammon, M. A. Bolshtyansky, D. G. Foursa, and A. N. Pilipetskii, "70.46 Tb/s over 7,600 km and 71.65 Tb/s over 6,970 km transmission in C+L band using coded modulation with hybrid constellation shaping and nonlinearity compensation," *Journal of Lightwave Technology*, vol. 36, no. 1, pp. 114–121, Jan. 2018.

[22] J. Yu, X. Zhou, M.-F. Huang, Y. Shao, D. Qian, T. Wang, M. Cvijetic, P. Magill, L. Nelson, M. Birk, S. Ten, H. B. Matthew, and S. K. Mishra, "17 Tb/s (161×114 Gb/s) polmux-RZ-8PSK transmission over 662 km of ultra-low loss fiber using C-band EDFA amplification and digital coherent detection," in *Proc. European Conference on Optical Communication (ECOC)*, Sep. 2008, p. Th.3.E.2.

[23] A. Sano, H. Masuda, T. Kobayashi, M. Fujiwara, K. Horikoshi, E. Yoshida, Y. Miyamoto, M. Matsui, M. Mizoguchi, H. Yamazaki, Y. Sakamaki, and H. Ishii, "69.1-Tb/s (432 × 171-Gb/s) C- and extended L-band transmission over 240 km using PDM-16-QAM modulation and digital coherent detection," in *Proc. Optical Fiber Communication Conference (OFC)*, Mar. 2010, p. PDPB7.

[24] D. Qian, M.-F. Huang, E. Ip, Y.-K. Huang, Y. Shao, J. Hu, and T. Wang, "101.7-Tb/s (370×294-Gb/s) PDM-128QAM-OFDM transmission over 3×55-km SSMF using pilot-based phase noise mitigation," in *Proc. Optical Fiber Communication Conference (OFC)*, Mar. 2011, p. PDPB5.

[25] A. Sano, T. Kobayashi, S. Yamanaka, A. Matsuura, H. Kawakami, Y. Miyamoto, K. Ishihara, and H. Masuda, "102.3-Tb/s (224 × 548-Gb/s) C- and extended L-band all-Raman transmission over 240 km using PDM-64QAM single carrier FDM with digital pilot tone," in *Proc. Optical Fiber Communication Conference (OFC)*, Mar. 2012, p. PDPSC.3.

[26] J. Renaudier, A. C. Meseguer, A. Ghazisaeidi, P. Tran, R. Rios-Müller, R. Brenot, A. Verdier, F. Blache, K. Mekhazni, B. Duval, H. Debregeas, M. Achouche, A. Boutin, F. Morin, L. Letteron, N. Fontaine, Y. Frignac, and G. Charlet, "First 100-nm

continuous-band WDM transmission system with 115Tb/s transport over 100km using novel ultra-wideband semiconductor optical amplifiers," in *Proc. European Conference on Optical Communication (ECOC)*, Sep. 2017, p. Th.PDP.A.3.

[27] J. M. Kahn and D. A. B. Miller, "Communications expands its space," *Nature Photonics*, vol. 11, no. 1, pp. 5–8, Jan. 2017.

[28] D. J. Richardson, J. M. Fini, and L. E. Nelson, "Space-division multiplexing in optical fibres," *Nature Photonics*, vol. 7, no. 5, pp. 354–362, Apr. 2013.

[29] S. Iano, T. Sato, S. Sentsui, T. Kuroha, and Y. Nishimura, "Multicore optical fiber," in *Proc. Optical Fiber Communication Conference (OFC)*, Mar. 1979, p. WB1.

[30] G. P. Agrawal, *Fiber-optic communications systems*, 3rd ed. Hoboken, NJ, USA: John Wiley & Sons, Inc., 2002.

[31] A. K. Majumdar, *Advanced Free Space Optics (FSO)*. New York City, NY, USA: Springer, 2015.

[32] K. Xu, D. Cheng, and X. Huang, "Multimode communication system used in local area network(LAN)," in *Proc. Symposium on Photonics and Optoelectronics (SOPO)*, Aug. 2009.

[33] A. M. Joshi, S. Datta, and A. Crawford, "Next-gen communications fiber: Multilevel modulation formats push capacities beyond 100 Gbit/s," *Laser Focus World*, vol. 48, no. 2, pp. 58–63, 2012.

[34] T. Miya, Y. Terunuma, T. Hosaka, and T. Miyashita, "Ultimate low-loss single-mode fibre at 1.55 μm," *IET Electronic Letters*, vol. 15, no. 4, pp. 106–108, Feb. 1979.

[35] B. G. Bathula, R. K. Sinha, A. L. Chiu, M. D. Feuer, G. Li, S. L. Woodward, W. Zhang, R. Doverspike, P. Magill, and K. Bergman, "Constraint routing and regenerator site concentration in ROADM networks," *IEEE/OSA Journal of Optical Communications and Networking*, vol. 5, no. 11, pp. 1202–1214, Nov. 2013.

[36] O. Gerstel, M. Jinno, A. Lord, and S. J. B. Yoo, "Elastic optical networking: A new dawn for the optical layer?" *IEEE Communications Magazine*, vol. 50, no. 2, pp. 12–20, Feb. 2012.

[37] R. H. Stolen and E. P. Ippen, "Raman gain in glass optical waveguides," *APL Applied Physics Letters*, vol. 22, no. 6, pp. 276–278, Mar. 1973.

[38] M. Secondini and E. Forestieri, "Scope and limitations of the nonlinear Shannon limit," *Journal of Lightwave Technology*, vol. 35, no. 4, pp. 893–902, Feb. 2017.

[39] G. Agrawal, *Nonlinear Fiber Optics*, 4th ed. New York City, NY, USA: Elsevier Science, 2007.

[40] A. Mecozzi and M. Shtaif, "The statistics of polarization-dependent loss in optical communication systems," *IEEE Photonics Technology Letters*, vol. 14, no. 3, pp. 313–315, Mar. 2002.

[41] B. Huttner, C. Geiser, and N. Gisin, "Polarization-induced distortions in optical fiber networks with polarization-mode dispersion and polarization-dependent losses," *IEEE Journal of Selected Topics in Quantum Electronics*, vol. 6, no. 2, pp. 317–329, Mar. 2000.

[42] T. Duthel, C. R. S. Fludger, J. Geyer, and C. Schulien, "Impact of polarisation dependent loss on coherent POLMUX-NRZ-DQPSK," in *Proc. Optical Fiber Communication Conference (OFC)*, Feb. 2008, p. OTh4E.3.

[43] M. P. Yankov, T. Fehenberger, L. Barletta, and N. Hanik, "Low-complexity tracking of laser and nonlinear phase noise in WDM optical fiber systems," *Journal of Lightwave Technology*, vol. 33, no. 23, pp. 4975–4984, Dec. 2015.

[44] X. Liu, A. R. Chraplyvy, P. J. Winzer, R. W. Tkach, and S. Chandrasekhar, "Phase-conjugated twin waves for communication beyond the Kerr nonlinearity limit," *Nature Photonics*, vol. 7, no. 7, pp. 560–568, May 2013.

[45] S. L. Jansen, D. van den Borne, P. M. Krummrich, S. Spälter, G.-D. Khoe, and H. de Waardt, "Long-haul DWDM transmission systems employing optical phase conjugation," *IEEE Journal of Selected Topics in Quantum Electronics*, vol. 12, no. 4, pp. 505–520, Jul. 2006.

[46] R.-J. Essiambre, P. J. Winzer, X. Q. Wang, W. Lee, C. A. White, and E. C. Burrows, "Electronic predistortion and fiber nonlinearity," *IEEE Photonics Technology Letters*, vol. 18, no. 17, pp. 1804–1806, Sep. 2006.

[47] E. Ip, "Nonlinear compensation using backpropagation for polarization-multiplexed transmission," *Journal of Lightwave Technology*, vol. 28, no. 6, pp. 939–951, Mar. 2010.

[48] F. Derr, "Coherent optical QPSK intradyne system: concept and digital receiver realization," *Journal of Lightwave Technology*, vol. 10, no. 9, pp. 1290–1296, Sep. 1992.

[49] K. Petermann, *Laser Diode Modulation and Noise*. Netherlands: Springer Netherlands, 1988.

[50] U. Madhow, *Fundamentals of Digital Communication*. New York City, NY, USA: Cambridge University Press, 2008.

[51] C. H. Henry, "Theory of the linewidth of semiconductor lasers," *IEEE Journal of Selected Topics in Quantum Electronics*, vol. 18, no. 2, pp. 259–264, Feb. 1982.

[52] W. Shieh and K.-P. Ho, "Equalization-enhanced phase noise for coherent-detection systems using electronic digital signal processing," *Optics Express*, vol. 16, no. 20, pp. 15 718–15 727, Sep. 2008.

[53] I. Fatadin, S. J. Savory, and D. Ives, "Compensation of quadrature imbalance in an optical QPSK coherent receiver," *IEEE Photonics Technology Letters*, vol. 20, no. 20, pp. 1733–1735, Oct. 2008.

[54] T.-H. Nguyen, P. Scalart, M. Joindot, M. Gay, L. Bramerie, C. Peucheret, A. Carer, J.-C. Simon, and O. Sentieys, "Joint simple blind IQ imbalance compensation and adaptive equalization for 16-QAM optical communications," in *Proc. IEEE International Conference on Communications (ICC)*, Jun. 2015, pp. 4913–4918.

[55] T. Tanimura, S. Oda, T. Tanaka, T. Hoshida, Z. Tao, and J. C. Rasmussen, "A simple digital skew compensator for coherent receiver," in *Proc. European Conference on Optical Communication (ECOC)*, Sep. 2009, p. 7.3.2.

[56] Y. Wang, E. Serpedin, and P. Ciblat, "An alternative blind feedforward symbol timing estimator using two samples per symbol," *IEEE Transactions on Communications*, vol. 51, no. 9, pp. 1451–1455, Sep. 2003.

[57] R. Dar and P. J. Winzer, "Nonlinear interference mitigation: Methods and potential gain," *Journal of Lightwave Technology*, vol. 35, no. 4, pp. 903–930, Feb. 2017.

[58] I. Mayer, "On Löwdin's method of symmetric orthogonalization," *International Journal of Quantum Chemistry*, vol. 90, no. 1, pp. 63–65, Feb. 2002.

[59] S. J. Savory, "Digital coherent optical receivers: Algorithms and subsystems," *IEEE Journal of Selected Topics in Quantum Electronics*, vol. 16, no. 5, pp. 1164–1179, Sep. 2010.

[60] S. H. Chang, H. S. Chung, and K. Kim, "Impact of quadrature imbalance in optical coherent QPSK receiver," *IEEE Photonics Technology Letters*, vol. 21, no. 11, pp. 709–711, Jun. 2009.

[61] C. S. Petrou, A. Vgenis, I. Roudas, and L. Raptis, "Quadrature imbalance compensation for PDM QPSK coherent optical systems," *IEEE Photonics Technology Letters*, vol. 21, no. 24, pp. 1876–1878, Dec. 2009.

[62] Y. Qiao, Y. Xu, L. Li, and Y. Ji, "Quadrature imbalance compensation algorithm based on statistical properties of signals in CO-QPSK system," *IEEE Chinese Optics Letters*, vol. 10, no. 12, pp. 120601-1–4, Dec. 2012.

[63] R. A. Soriano, F. N. Hauske, N. G. Gonzalez, Z. Zhang, Y. Ye, and I. T. Monroy, "Chromatic dispersion estimation in digital coherent receivers," *Journal of Lightwave Technology*, vol. 29, no. 11, pp. 1627–1637, Jun. 2011.

[64] S. J. Savory, "Digital filters for coherent optical receivers," *Optics Express*, vol. 16, no. 2, pp. 804–817, Jan. 2008.

[65] S. J. Savory, G. Gavioli, R. I. Killey, and P. Bayvel, "Electronic compensation of chromatic dispersion using a digital coherent receiver," *Optics Express*, vol. 15, no. 5, pp. 2120–2126, Mar. 2007.

[66] G. Goldfarb and G. Li, "Chromatic dispersion compensation using digital IIR filtering with coherent detection," *IEEE Photonics Technology Letters*, vol. 19, no. 13, pp. 969–971, Jul. 2007.

[67] M. Kuschnerov, F. N. Hauske, K. Piyawanno, B. Spinnler, M. S. Alfiad, A. Napoli, and B. Lankl, "DSP for coherent single-carrier receivers," *Journal of Lightwave Technology*, vol. 27, no. 16, pp. 3614–3622, Aug. 2009.

[68] F. N. Hauske, M. Kuschnerov, B. Spinnler, and B. Lankl, "Optical performance monitoring in digital coherent receivers," *Journal of Lightwave Technology*, vol. 27, no. 16, pp. 3623–3631, Aug. 2009.

[69] H. Wymeersch and P. Johannisson, "Maximum-likelihood-based blind dispersion estimation for coherent optical communication," *Journal of Lightwave Technology*, vol. 30, no. 18, pp. 2976–2982, Sep. 2012.

[70] F. Pittalà, F. N. Hauske, Y. Ye, N. G. Gonzalez, and I. T. Monroy, "Fast and robust CD and DGD estimation based on data-aided channel estimation," in *Proc. International Conference on Transparent Optical Networks (ICTON)*, Jun. 2011.

[71] C. Do, A. V. Tran, and D. F. Hewitt, "Chromatic dispersion estimation based on complementary golay sequences for 80 Gb/s QPSK single-carrier system with frequency domain equalization," in *Proc. Australasian Telecommunication Networks and Applications Conference (ATNAC)*, Nov. 2011.

[72] D. N. Godard, "Self-recovering equalization and carrier tracking in two-dimensional data communication systems," *IEEE Transactions on Communications*, vol. 28, no. 11, pp. 1867–1875, Nov. 1980.

[73] I. Fatadin, D. Ives, and S. J. Savory, "Blind equalization and carrier phase recovery in a 16-QAM optical coherent system," *Journal of Lightwave Technology*, vol. 27, no. 15, pp. 3042–3049, Aug. 2009.

[74] M. J. Ready and R. P. Gooch, "Blind equalization based on radius directed adaptation," in *Proc. International Conference on Acoustics, Speech, and Signal Processing (ICASSP)*, vol. 3, Apr. 1990, pp. 1699–1702.

[75] P. J. Winzer, A. H. Gnauck, C. R. Doerr, M. Magarini, and L. L. Buhl, "Spectrally efficient long-haul optical networking using 112-Gb/s polarization-multiplexed 16-QAM," *Journal of Lightwave Technology*, vol. 28, no. 4, pp. 547–556, Feb. 2010.

[76] A. Leven, N. Kaneda, U.-V. Koc, and Y.-K. Chen, "Frequency estimation in intradyne reception," *IEEE Photonics Technology Letters*, vol. 19, no. 6, pp. 366–368, Mar. 2007.

[77] S. Hoffmann, S. Bhandare, T. Pfau, O. Adamczyk, C. Wördehoff, R. Peveling, M. Porrmann, and R. Noé, "Frequency and phase estimation for coherent QPSK transmission with unlocked DFB lasers," *IEEE Photonics Technology Letters*, vol. 20, no. 18, pp. 1569–1571, Sep. 2008.

[78] M. Morelli and U. Mengali, "Feedforward frequency estimation for PSK: A tutorial review," *European Transactions on Telecommunications*, vol. 9, no. 2, pp. 103–116, Mar. 1998.

[79] M. Selmi, Y. Jaouën, and P. Ciblat, "Accurate digital frequency offset estimator for coherent PolMux QAM transmission systems," in *Proc. European Conference on Optical Communication (ECOC)*, Sep. 2009, p. P3.08.

[80] A. Alvarado, E. Agrell, D. Lavery, R. Maher, and P. Bayvel, "Replacing the soft-decision FEC limit paradigm in the design of optical communication systems," *Journal of Lightwave Technology*, vol. 33, no. 20, pp. 4338–4352, Oct. 2015.

[81] R. Gallager, "Low-density parity-check codes," *IRE Transactions on Information Theory*, vol. 8, no. 1, pp. 21–28, Jan. 1962.

[82] I. S. Reed and G. Solomon, "Polynomial codes over certain finite fields," *Journal of the Society for Industrial and Applied Mathematics*, vol. 8, no. 2, pp. 300–304, Jun. 1960.

[83] L. Schmalen, A. J. de Lind van Wijngaarden, and S. ten Brink, "Forward error correction in optical core and optical access networks," *Bell Labs Technical Journal*, vol. 18, no. 3, pp. 39–66, Dec. 2013.

[84] M. K. Simon and R. Annavajjala, "On the optimality of bit detection of certain digital modulations," *IEEE Transactions on Communications*, vol. 53, no. 2, pp. 299–307, Feb. 2005.

[85] C. Herzet, N. Noels, V. Lottici, H. Wymeersch, M. Luise, M. Moeneclaey, and L. Vandendorpe, "Code-aided turbo synchronization," *Proceedings of the IEEE*, vol. 95, no. 6, pp. 1255–1271, Jun. 2007.

[86] G. Colavolpe, A. Barbieri, and G. Caire, "Algorithms for iterative decoding in the presence of strong phase noise," *IEEE Journal on Selected Areas in Communications*, vol. 23, no. 9, pp. 1748–1757, Sep. 2005.

[87] W. Ryan and S. Lin, *Channel Codes: Classical and Modern*. Cambridge University Press, 2009.

[88] S. M. Kay, *Fundamentals of Statistical Signal Processing: Estimation Theory*. Upper Saddle River, NJ, USA: Prentice-Hall, Inc., 1993.

[89] A. P. Dempster, N. M. Laird, and D. B. Rubin, "Maximum likelihood from incomplete data via the EM algorithm," *Journal of the Royal Statistical Society. Series B (Methodological)*, vol. 39, no. 1, pp. 1–38, 1977.

[90] M. J. Beal, "Variational algorithms for approximate Bayesian inference," Ph.D. dissertation, University College London, 2003.

[91] F. R. Kschischang, B. J. Frey, and H.-A. Loeliger, "Factor graphs and the sum-product algorithm," *IEEE Transactions on Information Theory*, vol. 47, no. 2, pp. 498–519, Feb. 2001.

[92] A. Doucet, A. Smith, N. de Freitas, and N. Gordon, *Sequential Monte Carlo Methods in Practice*, ser. Information Science and Statistics. Springer New York, 2001.

[93] S. Särkkä, *Bayesian Filtering and Smoothing*, 1st ed. Cambridge, UK: Cambridge University Press, 2013.

[94] T. Pfau, S. Hoffmann, and R. Noé, "Hardware-efficient coherent digital receiver concept with feedforward carrier recovery for M-QAM constellations," *Journal of Lightwave Technology*, vol. 27, no. 8, pp. 989–999, Apr. 2009.

[95] A. J. Viterbi and A. M. Viterbi, "Nonlinear estimation of PSK-modulated carrier phase with application to burst digital transmission," *IEEE Transactions on Information Theory*, vol. 29, no. 4, pp. 543–551, Jul. 1983.

[96] E. Ip and J. M. Kahn, "Feedforward carrier recovery for coherent optical communications," *Journal of Lightwave Technology*, vol. 25, no. 9, pp. 2675–2692, Sep. 2007.

[97] M. Xiang, S. Fu, L. Deng, M. Tang, P. Shum, and D. Liu, "Low-complexity feedforward carrier phase estimation for M-ary QAM based on phase search acceleration by quadratic approximation," *Optics Express*, vol. 23, no. 15, pp. 19 142–19 153, Jul. 2015.

[98] C. Xie, S. Fu, J. Lu, L. Deng, M. Tang, and D. Liu, "Simplified blind phase search for low-complexity carrier phase estimation of M-ary QAM format," in *Proc. Asia Communications and Photonics Conference (ACPC)*, Nov. 2017, p. Su3B.6.

[99] T.-H. Nguyen, S.-P. Gorza, J. Louveaux, and F. Horlin, "Low-complexity blind phase search for filter bank multicarrier offset-QAM optical fiber systems," in *Proc. Signal Processing in Photonic Communications (SPPCom)*, Jul. 2016, p. SpW2G.2.

[100] F. Rice, M. Rice, and B. Cowley, "A new algorithm for 16QAM carrier phase estimation using QPSK partitioning," *Digital Signal Processing*, vol. 12, no. 1, pp. 77–86, Jan. 2002.

[101] Y. Mori, C. Zhang, K. Igarashi, K. Katoh, and K. Kikuchi, "Phase-noise tolerance of optical 16-QAM signals demodulated with decision-directed carrier-phase estimation," in *Proc. Optical Fiber Communication Conference (OFC)*, Mar. 2009.

[102] W. J. Weber, "Differential encoding for multiple amplitude and phase shift keying systems," *IEEE Transactions on Communications*, vol. 26, no. 3, pp. 385–391, Mar. 1978.

[103] E. R. Cacciamani and C. J. Wolejsza, "Phase-ambiguity resolution in a four-phase PSK communications system," *IEEE Transactions on Communications*, vol. 19, no. 6, pp. 1200–1210, Dec. 1971.

[104] H. Cheng, Y. Li, F. Zhang, J. Wu, J. Lu, G. Zhang, J. Xu, and J. Lin, "Pilot-symbols-aided cycle slip mitigation for DP-16QAM optical communication systems," *Optics Express*, vol. 21, no. 19, pp. 22 166–22 172, Sep. 2013.

[105] D. S. Millar, R. Maher, D. Lavery, T. Koike-Akino, M. Pajovic, A. Alvarado, M. Paskov, K. Kojima, K. Parsons, B. C. Thomsen, S. J. Savory, and P. Bayvel, "Design of a 1 Tb/s superchannel coherent receiver," *Journal of Lightwave Technology*, vol. 34, no. 6, pp. 1453–1463, Mar. 2016.

[106] R. Maher, K. Croussore, M. Lauermann, R. Going, X. Xu, and J. Rahn, "Constellation shaped 66 GBd DP-1024QAM transceiver with 400 km transmission over standard SMF," in *Proc. European Conference on Optical Communication (ECOC)*, Sep. 2017, p. Th.PDP.B.2.

[107] V. Kamalov, L. Jovanovski, V. Vusirikala, S. Zhang, F. Yaman, K. Nakamura, T. Inoue, E. Mateo, and Y. Inada, "Evolution from 8QAM live traffic to PS 64-QAM with neural-network based nonlinearity compensation on 11000 km open subsea cable," in *Proc. Optical Fiber Communication Conference (OFC)*, Mar. 2018, p. Th4D.5.

[108] J.-X. Cai, H. G. Batshon, M. V. Mazurczyk, O. V. Sinkin, D. Wang, M. Paskov, C. R. Davidson, W. W. Patterson, A. Turukhin, M. A. Bolshtyansky, and D. G. Foursa, "51.5 Tb/s capacity over 17,107 km in C+L bandwidth using single-mode fibers and nonlinearity compensation," *Journal of Lightwave Technology*, vol. 36, no. 11, pp. 2135–2141, Jun. 2018.

[109] A. Ghazisaeidi, I. F. de Jauregui Ruiz, R. Rios-Muller, L. Schmalen, P. Tran, P. Brindel, A. C. Meseguer, Q. Hu, F. Buchali, G. Charlet, and J. Renaudier, "65Tb/s transoceanic transmission using probabilistically-shaped PDM-64QAM," in *Proc. European Conference on Optical Communication (ECOC)*, Sep. 2016, p. Th.3.C.4.

[110] N. Noels, J. Bhatti, H. Bruneel, and M. Moeneclaey, "Block-processing soft-input soft-output demodulator for coded PSK using DCT-based phase noise estimation," *IEEE Transactions on Communications*, vol. 62, no. 8, pp. 2939–2950, Aug. 2014.

[111] M. Nissilä and S. Pasupathy, "Adaptive iterative detectors for phase-uncertain channels via variational bounding," *IEEE Transactions on Communications*, vol. 57, no. 3, pp. 716–725, Mar. 2009.

[112] A. F. Alfredsson, R. Krishnan, and E. Agrell, "Joint-polarization phase-noise estimation and symbol detection for optical coherent receivers," *Journal of Lightwave Technology*, vol. 34, no. 18, pp. 4394–4405, Sep. 2016.

[113] R. E. Kalman, "A new approach to linear filtering and prediction problems," *ASME Journal of Basic Engineering*, vol. 82, no. 1, pp. 35–45, Mar. 1960.

[114] M. Pajovic, D. S. Millar, T. Koike-Akino, R. Maher, D. Lavery, A. Alvarado, M. Paskov, K. Kojima, K. Parsons, B. C. Thomsen, S. J. Savory, and P. Bayvel, "Experimental demonstration of multi-pilot aided carrier phase estimation for DP-64QAM and DP-256QAM," in *Proc. European Conference on Optical Communication (ECOC)*, Sep. 2015, p. Mo.4.3.3.

[115] R. Krishnan, M. R. Khanzadi, T. Eriksson, and T. Svensson, "Soft metrics and their performance analysis for optimal data detection in the presence of strong oscillator phase noise," *IEEE Transactions on Communications*, vol. 61, no. 6, pp. 2385–2395, Jun. 2013.

[116] M. D. Feuer, L. E. Nelson, X. Zhou, S. L. Woodward, R. Isaac, B. Zhu, T. F. Taunay, M. Fishteyn, J. M. Fini, and M. F. Yan, "Joint digital signal processing receivers for spatial superchannels," *IEEE Photonics Technology Letters*, vol. 24, no. 21, pp. 1957–1960, Nov. 2012.

[117] R. G. H. van Uden, C. M. Okonkwo, V. A. J. M. Sleiffer, M. Kuschnerov, H. de Waardt, and A. M. J. Koonen, "Single DPLL joint carrier phase compensation for few-mode fiber transmission," *IEEE Photonics Technology Letters*, vol. 25, no. 14, pp. 1381–1384, Jul. 2013.

[118] A. C. Bordonalli, M. J. Fice, and A. J. Seeds, "Optical injection locking to optical frequency combs for superchannel coherent detection," *Optics Express*, vol. 23, no. 2, pp. 1547–1557, Jan. 2015.

[119] D. V. Souto, B.-E. Olsson, C. Larsson, and D. A. A. Mello, "Joint-polarization and joint-subchannel carrier phase estimation for 16-QAM optical systems," *Journal of Lightwave Technology*, vol. 30, no. 20, pp. 3185–3191, Oct. 2012.

[120] B. J. Puttnam, J. Sakaguchi, J.-M. Delgado Mendinueta, W. Klaus, Y. Awaji, N. Wada, A. Kanno, and T. Kawanishi, "Investigating self-homodyne coherent detection in a 19 channel space-division-multiplexed transmission link," *Optics Express*, vol. 21, no. 2, pp. 1561–1566, Jan. 2013.

[121] A. Lorences-Riesgo, T. A. Eriksson, A. Fülöp, P. A. Andrekson, and M. Karlsson, "Frequency-comb regeneration for self-homodyne superchannels," *Journal of Lightwave Technology*, vol. 34, no. 8, pp. 1800–1806, Apr. 2016.

[122] R. S. Luís, B. J. Puttnam, J.-M. Delgado Mendinueta, W. Klaus, Y. Awaji, and N. Wada, "Comparing inter-core skew fluctuations in multi-core and single-core fibers," in *Proc. Conference on Lasers and Electro-Optics (CLEO)*, May 2015, p. SM2L.5.

[123] K. Cho and D. Yoon, "On the general BER expression of one- and two-dimensional amplitude modulations," *IEEE Transactions on Communications*, vol. 50, no. 7, pp. 1074–1080, Jul. 2002.

[124] R. Krishnan, G. Colavolpe, A. Graell i Amat, and T. Eriksson, "Algorithms for joint phase estimation and decoding for MIMO systems in the presence of phase noise and quasi-static fading channels," *IEEE Transactions on Signal Processing*, vol. 63, no. 13, pp. 3360–3375, Jul. 2015.

[125] A. O. Isikman, H. Mehrpouyan, A. A. Nasir, A. Graell i Amat, and R. A. Kennedy, "Joint phase noise estimation and data detection in coded multi-input–multi-output systems," *IET Communications*, vol. 8, no. 7, pp. 981–989, May 2014.

[126] H. Mehrpouyan, A. A. Nasir, S. D. Blostein, T. Eriksson, G. K. Karagiannidis, and T. Svensson, "Joint estimation of channel and oscillator phase noise in MIMO systems," *IEEE Transactions on Signal Processing*, vol. 60, no. 9, pp. 4790–4807, Sep. 2012.

[127] R. S. Luís, B. J. Puttnam, J.-M. Delgado Mendinueta, Y. Awaji, and N. Wada, "Impact of spatial channel skew on the performance of spatial-division multiplexed self-homodyne transmission systems," in *Proc. International Conference on Photonics in Switching (PS)*, Sep. 2015, pp. 37–39.

[128] B. J. Puttnam, T. A. Eriksson, J.-M. Delgado Mendinueta, R. S. Luís, Y. Awaji, N. Wada, M. Karlsson, and E. Agrell, "Modulation formats for multi-core fiber transmission," *Optics Express*, vol. 22, no. 26, pp. 32 457–32 469, Dec. 2014.

[129] B. J. Puttnam, R. S. Luís, W. Klaus, J. Sakaguchi, J.-M. Delgado Mendinueta, Y. Awaji, N. Wada, Y. Tamura, T. Hayashi, M. Hirano, and J. Marciante, "2.15 Pb/s transmission using a 22 core homogeneous single-mode multi-core fiber and wideband optical comb," in *Proc. European Conference on Optical Communication (ECOC)*, Sep. 2015, p. PDP.3.1.

[130] A. Turukhin, H. G. Batshon, M. Mazurczyk, Y. Sun, C. R. Davidson, J.-X. Chai, O. V. Sinkin, W. Patterson, G. Wolter, M. A. Bolshtyansky, D. G. Foursa, and A. Pilipetskii, "Demonstration of 0.52 Pb/s potential transmission capacity over 8,830 km using multicore fiber," in *Proc. European Conference on Optical Communication (ECOC)*, Sep. 2016, p. Tu.1.D.3.

[131] M. Koshiba, K. Saitoh, and Y. Kokubun, "Heterogeneous multi-core fibers: proposal and design principle," *IEICE Electronic Express*, vol. 6, no. 2, pp. 98–103, Jan. 2009.

[132] T. Mizuno, K. Shibahara, F. Ye, Y. Sasaki, Y. Amma, K. Takenaga, Y. Jung, K. Pulverer, H. Ono, Y. Abe, M. Yamada, K. Saitoh, S. Matsuo, K. Aikawa, M. Bohn, D. J. Richardson, Y. Miyamoto, and T. Morioka, "Long-haul dense space-division multiplexed transmission over low-crosstalk heterogeneous 32-core transmission line using a partial recirculating loop system," *Journal of Lightwave Technology*, vol. 35, no. 3, pp. 488–498, Feb. 2017.

[133] T. Sakamoto, T. Mori, M. Wada, T. Yamamoto, F. Yamamoto, and K. Nakajima, "Strongly-coupled multi-core fiber and its optical characteristics for MIMO transmission systems," *Optical Fiber Technology*, vol. 35, pp. 8–18, Feb. 2017.

[134] J.-I. Sakai, K. Kitayama, M. Ikeda, Y. Kato, and T. Kimura, "Design considerations of broadband dual-mode optical fibers," *IEEE Transactions on Microwave Theory and Techniques*, vol. 26, no. 9, pp. 658–665, Sep. 1978.

[135] S. Ö. Arık, K.-P. Ho, and J. M. Kahn, "Optical network scaling: roles of spectral and spatial aggregation," *Optics Express*, vol. 22, no. 24, pp. 29 868–29 887, Dec. 2014.

[136] C. Antonelli, O. Golani, M. Shtaif, and A. Mecozzi, "Nonlinear interference noise in space-division multiplexed transmission through optical fibers," *Optics Express*, vol. 25, no. 12, pp. 13 055–13 078, Jun. 2017.

[137] N. K. Fontaine, R. Ryf, H. Chen, A. Velazquez Benitez, J. E. Antonio Lopez, R. Amezcua Correa, B. Guan, B. Ercan, R. P. Scott, S. J. Ben Yoo, L. Grüner-Nielsen, Y. Sun, and R. J. Lingle, "30×30 MIMO transmission over 15 spatial modes," in *Proc. Optical Fiber Communication Conference (OFC)*, Mar. 2015, p. Th5C.1.

[138] K. Igarashi, D. Souma, Y. Wakayama, K. Takeshima, Y. Kawaguchi, T. Tsuritani, I. Morita, and M. Suzuki, "114 space-division-multiplexed transmission over 9.8-km weakly-coupled-6-mode uncoupled-19-core fibers," in *Proc. Optical Fiber Communication Conference (OFC)*, Mar. 2015, p. Th5C.4.